UNCLASSIFIED

Defense Threat Reduction Agency
Research and Development
Counter WMD Technologies
Test Support Division
1680 Texas Street SE
Kirtland AFB, NM 87117-5669

DTRA FTR-17-003

FINAL TEST REPORT

REVEAL Data Analysis Results from 2016 Jack Rabbit II Field Testing

June 2017

Distribution A: Approved for public release: distribution unlimited.

Trade Names Statement: The use of trade names in this document does not constitute an official endorsement or approval of the use of such commercial hardware or software. This document may not be cited for purposes of advertisement.

Author: Patrick Ponsardin
Spectral Sensor Solutions, LLC

Technical Monitor: Bruce Hinds
DTRA/J9 Test Support Division

REPORT DOCUMENTATION PAGE

Form Approved
OMB No. 0704-0188

1. REPORT DATE *(DD-MM-YYYY)*
30 June 2017

2. REPORT TYPE
Final Test Report

3. DATES COVERED *(From-To)*
27 August 2016 to 30 June 2017

4. TITLE AND SUBTITLE
REVEAL Data Analysis Results from 2016 Jack Rabbit II Field Testing DTRA FTR-17-003

5a. CONTRACT NUMBER
HDTRA2-16-C-0001

5b. GRANT NUMBER

5c. PROGRAM ELEMENT NUMBER

5d. PROJECT NUMBER

5e. TASK NUMBER

5f. WORK UNIT NUMBER

6. AUTHORS

Author: Patrick L. Ponsardin
Spectral Sensor Solutions, LLC.

Technical Monitor: Bruce Hinds
Defense Threat Reduction Agency

7. PERFORMING ORGANIZATION NAME(S) AND ADDRESS(ES)

Defense Threat Reduction Agency
1680 Texas St. SE, Building 20363
Kirtland AFB, NM 87117-5669

Spectral Sensor Solutions, LLC
2613 Paddock Gate Ct
Herndon, VA 20171

8. **PERFORMING ORGANIZATION REPORT NUMBER**
DTRA FTR-17-003

9. SPONSORING/MONITORING AGENCY NAME(S) AND ADDRESS(ES)

Defense Threat Reduction Agency
8725 John J. Kingman Road
Fort Belvoir, VA 22060-6201

10. SPONSOR/MONITOR'S ACRONYM(S)

11. SPONSOR/MONITOR'S REPORT No.

12. DISTRIBUTION/AVAILABILITY STATEMENT
Distribution A: Approved for public release; distribution unlimited.

13. SUPPLEMENTARY NOTES

14. ABSTRACT

Spectral Sensor Solutions (S3) deployed two eye-safe elastic backscatter lidar systems in support of the Jack Rabbit II – 2016 field experiment. The Real-time Eye-safe Visualization, Evaluation, and Analysis Lidar (REVEAL) technology is capable of simultaneously mapping/tracking aerosol plumes and deriving the 2-D horizontal wind vectors from the aerosol motion. The two systems, REVEAL-Prototype and REVEAL-5000, successfully collected chlorine aerosol relative concentration data from all four JRII – 2016 chlorine releases. This data includes measurements of aerosol distributions in the plume jet region, measurements of the maximum height of a vertically released plume, an estimate of aerosol plume touch down location and time for the vertical plume and estimates of when the chlorine aerosols intercepted the aerosol point sensor station for all releases. Wind fields were also derived for some of the releases and example wind data is also presented.

15. SUBJECT TERMS
REVEAL Data Analysis Results from 2016 Jack Rabbit II Field Testing DTRA FTR-17-003, Real-time Eye-safe Visualization, Evaluation, and Analysis Lidar, REVEAL, lidar, chlorine aerosol, mapping, relative concentration, plume jet region

16. SECURITY CLASSIFICATION OF:			17. LIMITATION OF ABSTRACT	18. NUMBER OF PAGES	19a. NAME OF RESPONSIBLE PERSON:
					Bruce Hinds
a. REPORT	b. ABSTRACT	c. THIS PAGE	SAR	72	19b. TELEPHONE NUMBER *(include area code)*
UNCLASSIFIED	UNCLASSIFIED	UNCLASSIFIED			505-853-5722

Standard Form 298 (Rev. 8-98)
Prescribed by ANSI Std. 239.18

Table of Contents

List of Figures

List of Tables

1.0 Introduction

1.1 Background

The Department of Homeland Security (DHS) Chemical Security Analysis Center (CSAC) project Jack Rabbit II (JRII) consists of a series of large-scale outdoor chlorine release experiments that were conducted in 2015 and again during August and September of 2016 over the flat desert playa at Dugway Proving Ground (DPG), Utah. Spectral Sensor Solutions (S3) deployed two eye-safe elastic aerosol-backscatter lidar systems called Real-time Eye-safe Visualization, Evaluation, and Analysis Lidar (REVEAL) to provide additional data supporting the characterization of the releases. The first system, REVEAL-Prototype is the first generation system and was deployed in previous test fields at DPG. The second system, REVEAL-5000 is a more highly engineered version of the REVEAL and was developed and integrated just prior to these tests. The REVEAL-Prototype was in operation and collected data during the four releases that occurred on 31 August 2016 (JRII-6), 3 September 2016 (JRII-7), 11 September 2016 (JRII-8), and 17 September 2016 (JRII-9). The REVEAL-5000 was deployed later and collected data during JRII-8.

1.2 Objectives

Characterization of the aerosol content of the chlorine plume is important for a variety of reasons. Measurements of the formation, transport and dispersion, and fate of the chlorine aerosols could provide valuable insights into the dynamics of the plume and improve the results of the mixed phase models used to increase our understanding of the nature of the threat. The REVEAL can contribute to the characterization of the chlorine plume on a large scale by mapping and tracking the associated aerosol content of the release as it disperses in the surrounding environment. REVEAL also can contribute to the characterization of the chlorine release on a smaller scale by mapping the jet source at the chlorine release point and in the area immediately surrounding the release point.

The initial objectives of these measurements were as follows:

1. To provide measurements of the relative concentration of the aerosol component of the chlorine plume
2. To provide both the micro-scale wind information within the plume and the wide area wind fields around the plume
3. To provide a better understanding of the jet source at the release point

2.0 Methods, Assumptions, and Procedures

2.1 REVEAL System Description

The REVEAL system is an eye-safe elastic backscatter lidar operating at a wavelength of 1.5 µm (Figure 2-1) that has the capability to detect, map, and track aerosol plumes as well as measure the horizontal vector wind fields associated with the plume. This technology can significantly improve the characterization of the dynamics of the chlorine plume itself as well as the dynamics of the atmospheric environment in which the plume evolves. While REVEAL is not able to measure the absolute concentration of chlorine aerosols, it can measure the relative concentration at a high spatial resolution. Ranges of 5 km and up are achievable at nighttime but daylight backgrounds limit the maximum ranges to a couple of kilometers during daytime.

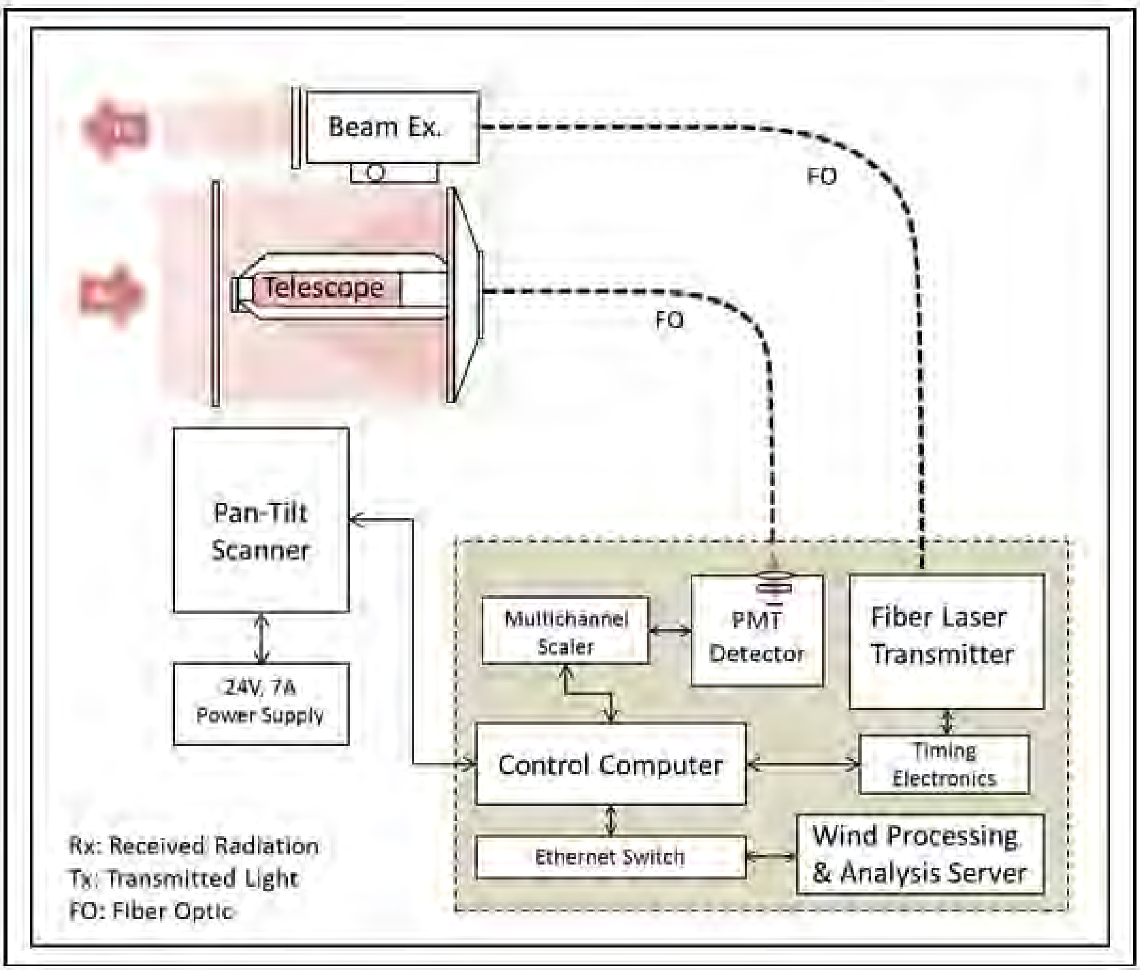

Figure 2-1. REVEAL system configuration identifying the various components

REVEAL counts the backscattered (180°) photons from aerosols in the path of the laser beam. The photo-counts level of the backscattered light is determined by the system parameters (primarily laser power, collection optic diameter, and detector sensitivity and noise), the backscatter cross section of the aerosols, and the extinction coefficient defined by other compounds of the surrounding atmosphere. The backscatter cross section is a highly varying quantity determined by the complex index of refraction, size, and shape of the aerosol. All of these variables, and in many cases unknowns, mean that REVEAL is not able to measure absolute quantitative concentration of the aerosols and instead provides a relative concentration value. Assuming a uniform type of aerosol, high photo counts correlate with high aerosol loading, while low photo counts signify atmospheric conditions with low aerosol loading.

Recent algorithm advancements have enabled the derivation of two-dimensional (2-D) vector wind-field measurements from REVEAL aerosol images, thus providing a second valuable meteorological data set. Wind fields are derived by comparing the positon of aerosol features in each successive scan (or frame). Spatial resolution of the wind vectors is a complex question because image processing techniques are used and multiple “pixels” in the aerosol features contribute to the resolution. Current estimates are that the spatial resolution of the wind vectors is ~25 m. Speed and direction accuracy are still under investigation, but comparisons with DPG anemometer data from the (Sophos/Kydoimos) S/K Challenge II field experiment in 2015 showed good correlation between the REVEAL and anemometer measurements. Current estimates are ±0.5 m/s for wind speed and ±3° for wind direction.

REVEAL operates at 15 kHz or 10 kHz pulse repetition frequency (PRF). Both systems were set to 10 kHz to minimize the range fold-over interferences with the data of interest (2 to 4 km). At 15 kHz, mountains located at 10 km or beyond will generate hard-target signals that will fold over and overlay the near field signals of the next lidar return.

REVEAL relies on photon counting within each range bin to generate a range resolved lidar return. In normal operation, 1500 laser pulses are accumulated to produce a lidar return histogram (photo counts versus range). These aerosol backscatter histograms extend to 10 km and are generated at 6.7 Hz while scanning.

Each histogram is saved to a binary file (.bscan) with a header containing the time (UTC), the sensor pointing direction (azimuth, elevation), the date, and the sensor location (latitude, longitude).

2.2 REVEAL Spatial Resolution and Scanning

REVEAL can scan horizontally between –180° and +180°. This field of regard (FOR) is in practice limited by the line of sight provided by the deployment platform. For the sensor deployment configuration used during the JRII tests, the back of the trailer provided a maximum horizontal FOR of –70° to +70°.

The scanner is set up to scan clockwise at the speed programmed by the operator. These forward scans can be at speeds of up to 20°/s. Once the forward scan is completed, the scanner flies back to the starting position at a maximum speed of 40°/s in order to minimize the time between scans. This temporal saw tooth scan pattern is needed by the wind retrieval algorithm, ensuring that all spatial elements of two successive scans are collected with the same time differential. The radial (line-of-sight) resolution is primarily determined by the range bin size and is set at 7.67 m.

The elemental lidar data is a voxel (volume element) corresponding to the number of backscattered photons from a volume located at a given range and a given pointing direction from the sensor. As is, the data can be displayed directly in the form of a Range Time Indicator (RTI), where range-resolved returns are color coded and stacked parallel in order of arrival to create a 2-D plot.

To create a dimensionally correct representation of the data, the sector scan data associated with horizontal scans are displayed as Plan Position Indicators (PPIs) where the range and bearing (azimuth angle) information are used to position each voxel as color-coded pixels in a radial or Cartesian 2-D plot.

REVEAL can also scan vertically between –10° and +70°. The sector scan data associated with vertical scans are displayed as Range Height Indicators (RHIs), where the range and elevation information are used to position each voxel as color-coded pixels in a radial or Cartesian 2-D plot.n.

Table 2-1 shows the typical voxel dimensions associated with the JRII scan over the release pad. One sensor configuration trade that requires special attention is spatial coverage versus spatial resolution versus frame rate. We define frame rate as the rate that a given scan pattern is repeated. It provides the sensor large-scale sampling rate associated with a release event. In order to achieve high angular resolution (i.e., the scanner motion during a histogram generation is small), low angular speeds are required, which translates into large repeat intervals for a given sector scan. So on one end, minimizing the spatial coverage (e.g., setting start and stop angles with minimum separation) and minimizing the spatial resolution (e.g., setting high scan speeds) provides the highest frame rates to best capture fleeting phenomena but also results in poor spatial information. On the other end, maximizing spatial coverage and maximizing spatial resolution provides the richest spatial information but results in slow frame rates unsuitable for highly dynamic events. During JRII we tried several combinations to optimize this trade off. The configuration used in the first test was evaluated in light of the collected data and deemed too spatially coarse. In the subsequent tests, the spatial resolution was increased while lowering the frame rates.

Table 2-1. Voxel size and frame rate settings for the PPI scans used over the release pad

Test	PPI Angular Span (°)	Angular Speed (°/s)	Voxel Size at 3 km (W × R × H) (m)	PPI Frame Rate (Hz)
JRII-6	1.5	0.40	3.65 × 7.7 × 0.45	0.22
JRII-7	2	0.10	1.25 × 7.7 × 0.45	0.05
JRII-8	2	0.20	2.05 × 7.7 × 0.45	0.1
JRII-9	3	0.30	2.85 × 7.7 × 0.45	0.1

The width (perpendicular to the line of sight and in the scanning plane) of the illuminated voxel at a given range is defined by the laser beam diameter at that range, and the angular scan during one histogram accumulation. The radial length (along the line of sight) of the illuminated voxel is defined by the laser-pulse length and the integration range-bin used to count backscatter photons. The height (perpendicular to the line of sight and in a plane perpendicular to the scanning plane) of the illuminated voxel is defined by the laser beam diameter at that range. The laser beam diverges at 120 microradians, and the beam diameter above the release pad reaches 0.45 m.

2.3 REVEAL Deployment Location

The REVEAL system was integrated inside a "toy hauler" trailer (Figure 2-2), and the back door was opened to provide direct line of sight of the targets of interest. The trailer was positioned directly on the playa, north of the command post (CP) and pointing westward directly to the release pad.

Table 2-2 provides the sensor coordinates as well as the relative distance and bearing of the release point and aerosol station with respect to the sensor. The last two columns provide the relative positions of these two components in Cartesian coordinates centered on the REVEAL sensor. These coordinates are used in most PPIs presented (see Figure 2-3 for details on XY coordinates of the release point).

Figure 2-2. REVEAL-Prototype integrated inside a trailer at DPG

To ensure proper calibration of the scanner angular sensor, the REVEAL laser beam expander was coupled to a visible red laser. The beam location was then inspected on the release pad to confirm that with the proper bearing dialed on the scanner (i.e., 268.30°), the sensor line of sight overlapped the release point location.

Following the calibration standard procedure, the GPS coordinates of the sensor and the scanner pointing offset were measured and logged in the control software so that all of the data files generated on location would have the proper header values.

On 1 April 2017, after reviewing the respective coordinates of the REVEAL sensor and the pad center, is was noted that the absolute calibration of the scanner pointing direction was off by 1.65°. The published bearing corresponding to the pad center should be 269.96° instead of 268.31°. The relative locations of the targets does not change but the Y axis values seen on the PPI scans should be all shifted by +88 m. In all the tables and figures seen below, we did not correct for this angular calibration error, but all absolute coordinates published in this report have been corrected to account for this error.

Table 2-2. REVEAL sensor, release point, and aerosol station relative positions

Component	Absolute Location		Position Relative to REVEAL Sensor			
	Latitude	Longitude	Range (m)	Bearing	X (m)	Y (m)
REVEAL	40.135162°	–113.451375°	0	*n/a*	0	0
Release point	40.134347°	–113.487076°	3053	268.31°	–3052	–90
Aerosol station	40.134825°	–113.487242°	3065	269.32°	–3065	–36

The exact height above ground of the sensor laser beam is difficult to estimate because temperature gradients result in beam bending as it propagates towards the release pad. The elevation angle was adjusted to ensure the beam was touching ground beyond 5 km. In the early mornings after daylight break, this resulted in an elevation angle of ~0.11°. This corresponded to an average height above the release pad of ~3 to 6 m.

For most releases, the sensor was configured for a narrow PPI scan (~2°) corresponding to a PPI scan type 1 in Figure 2-3. Once the release was started, the sensor was switched after a couple of minutes to a broader PPI scan (~30°) corresponding to a PPI scan type 2 in Figure 2-3.

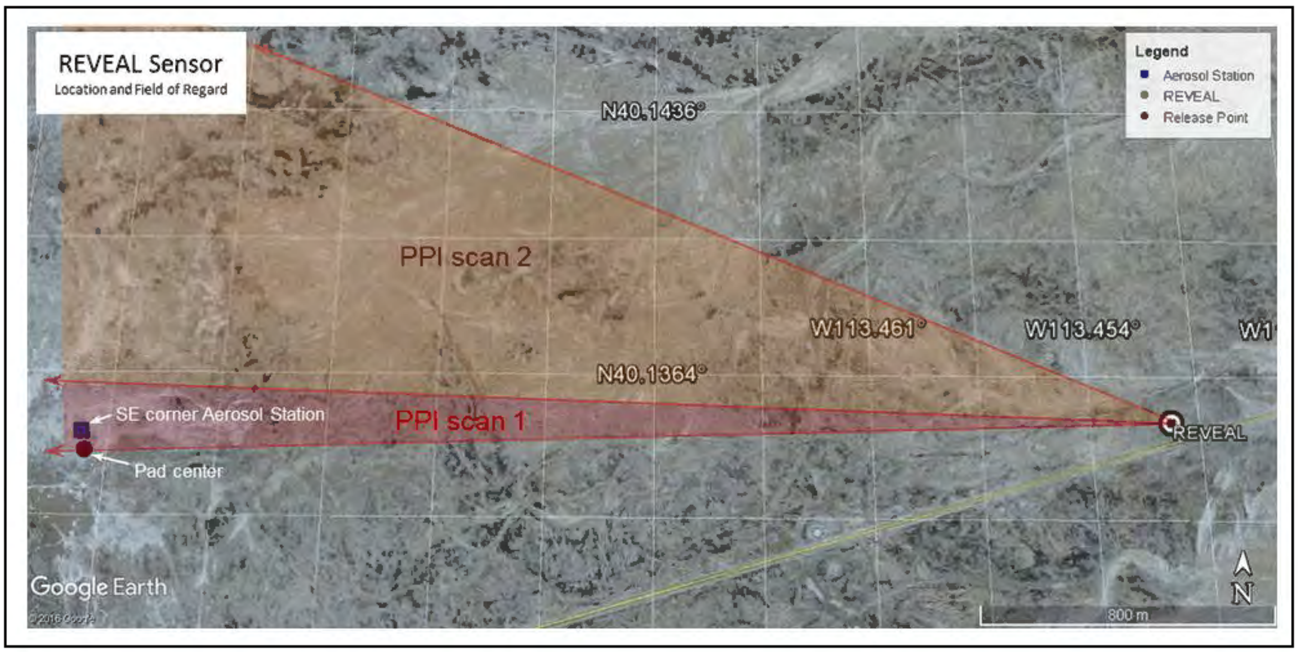

Figure 2-3. Layout of the REVEAL system and its FOR relative to the release area

PPI scans type 1 were setup specifically to monitor the detailed aerosol relative concentration structures near the release point in the minutes following the release. As such, these short scan sectors (1.5° to 3°) were able to provide the voxels sizes and repeat rates listed in Table 2-1 above the pad.

PPI scans type 2 were setup to provide a broader view of the aerosol cloud escaping the release pad. The angular scan speeds associated with these scan patterns were on the order of 2°/s, resulting in a voxel size (W × R × H) of ~20m × 7.7m × 0.45m at 3 km.

3.0 Results

The REVEAL-Prototype system participated in all the 2016 JRII tests, and the REVEAL-5000 system participated in a subset of these tests, providing complementary data for the JRII-8 test.

A detailed description of the collected data is provided in the following sections. Each section starts with a summary table giving a quick look of the sensor configuration for that specific test. Following that quick look table, the raw collected data, such as PPI or RHI images are provided for reference.

All the tests are presented in chronological order, even though REVEAL data collected during test 8 and test 9 provide the most interesting results. For JRII-8 and JRII-9, besides presenting the PPI and RHI data, additional analyses have been carried out to provide secondary data products of interest such as touch down location, plume height distribution, or cloud propagation speed.

3.1 JRII-6 Test

Table 3-1. JRII-6 REVEAL configuration quick look summary

Parameter	Value	
Date	31 Aug 2016	
Release start (local time)	08:23:35	
Release stop (local time)	08:24:30	
Released Cl_2 weight (lb)	18,460	
Release orientation from vertical (°)	180	
Wind direction (°)	160	
Wind speed (m/s)	2.3	
REVEAL-Prototype status	On site / collecting data	
REVEAL-Prototype scan pattern	PPI scan type 1 at 0.11° elevation	
	Start time	08:00:00
	Stop time	08:28:06
	Start angle	268.37°
	Stop angle	269.74°
	Angular speed	0.403°/s
	PPI scan type 2 at 0.11° elevation	
	Start time	08:28:21
	Stop time	08:41:03
	Start angle	270.07°
	Stop angle	300.27°
	Angular speed	3°/s
REVEAL-5000 status	Not on site	

3.1.1 PPI Type 1 Scans

For the first 4.5 min of this test, REVEAL-Prototype collected type 1 PPIs every 4.65 s including scanner fly-back time (Figure 3-1).

Figure 3-1 is composed of six vignettes representing PPI scans collected over the release pad, each spanning 1.4°. This represents a south–north measured sweep length of 80 m at a range of 3050 m from the REVEAL sensor. Each vignette is a zoomed portion of the collected scan, covering an area of 750 m × 850 m north of the release point. The top left vignette in Figure 3-1 has a red mark representing the release point location at x = –3044 m and y = –85 m.

The start of the PPI collection time (UTC) is provided above each vignette. The sweep starts from the southernmost point and proceeds clockwise towards the northernmost point. This forward sweep is accomplished in 3.3 s.

The elevation of 0.11° represented a height above the ground of more than 3 m estimated from the touch down location of the laser beam. This is higher than a standard freight container, and in these vignettes only the hard-target footprint of two of the video towers are visible. These are represented by the two white squares in each vignette.

The release of Cl_2 occurred at 14:23:35 UTC with a release direction of 180° from the vertical.

In all the vignettes a faint north/south plume in the middle of the zoomed area is visible. This is believed to be an aerosol plume generated by the wind blowing over the access road south of the release pad.

The middle right vignette and the bottom two vignettes from Figure 3-1 show a plume that might be attributed to the Cl_2 release. This plume emerges on the lidar scan sweep at the southwest corner of the north tower and propagates towards the north in the two subsequent vignettes. This plume disappears on the subsequent frames (not shown in this report) and no other features were detectable.

By tracking the plume location between the two last frames shown in Figure 3-1 and assuming this is the same plume (Figure 3-2), the released aerosol cloud ground speed can be estimated. Between the two frames, the plume has traveled 17.9 m, providing therefore an estimated plume ground speed of 3.8 m/s and a heading of 20° at that particular location. This aerosol cloud ground speed is significantly higher than the anemometer-measured wind speed of 2.8 m/s.

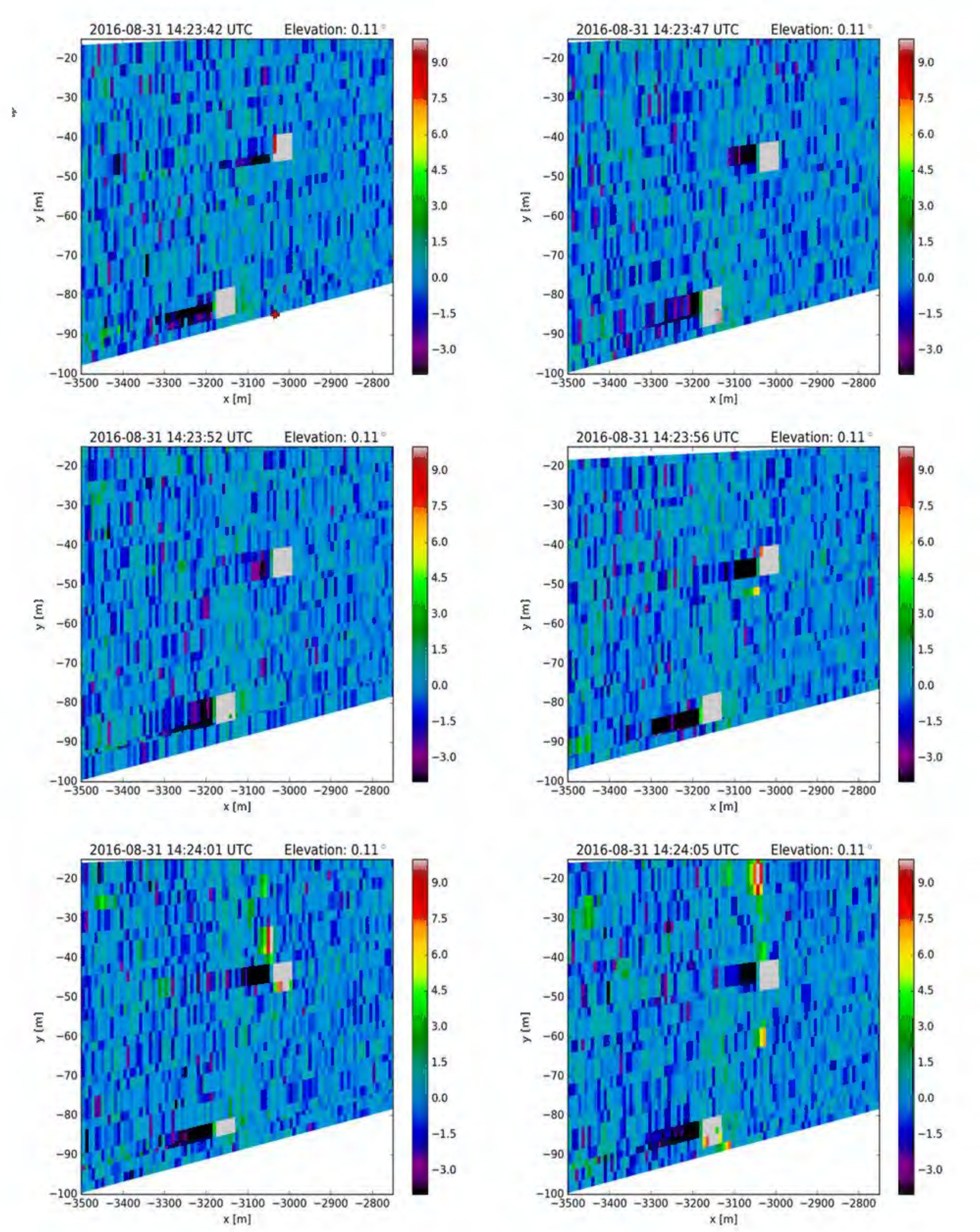

Figure 3-1. PPI scans above the release pad during the JRII-6 test. UTC time on top of each graph is start time of the scan; stop time of the scan is 3.3 s later.

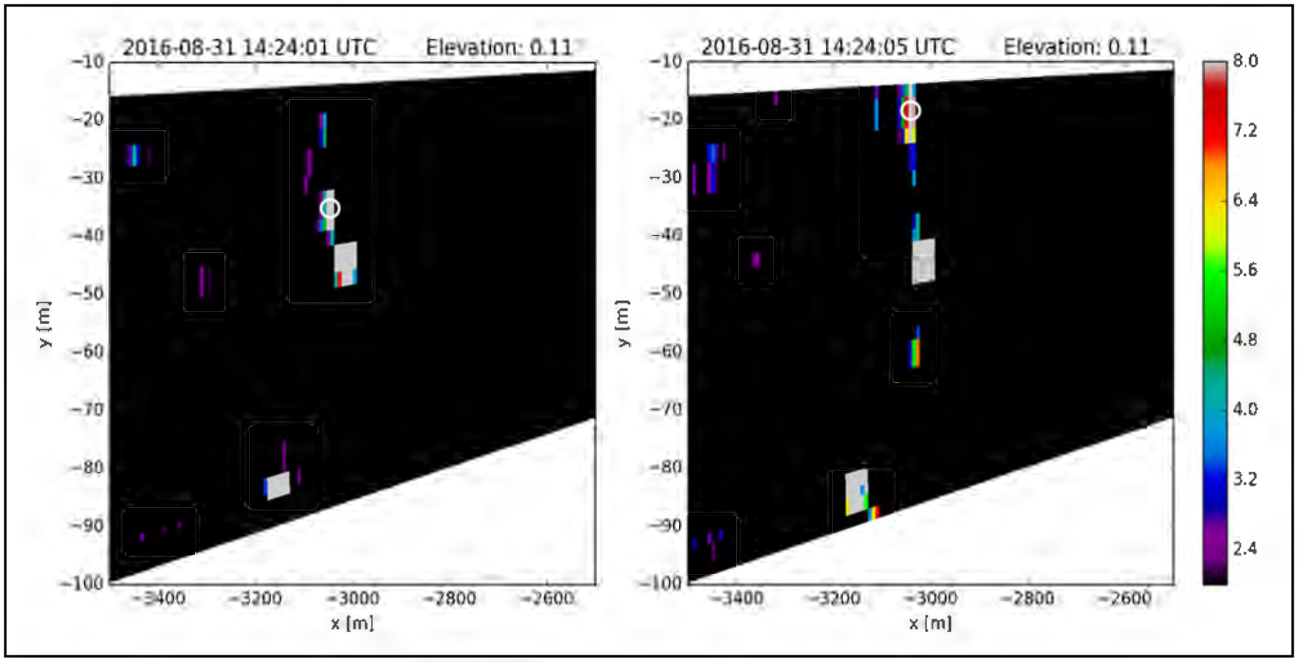

Figure 3-2. Last two frames from Figure 3-1 (JRII-6) showing the two sequences used to compute an aerosol cloud ground speed of 3.8 m/s at 14:24:04 UTC

3.1.2 PPI Type 2 Scans

After these initial type 1 data collections, the system was switched to type 2 PPIs that provided 30° scans north of the release point. The elevation angle was kept the same (0.11°) but due to the positioning of the sensor platform, the corresponding laser beam height above ground increased significantly.

The first type 2 PPI collected had a higher angular resolution due to the inadvertent low setting of the scanner angular speed (0.8°/s). This particular PPI (Figure 3-3) required 40 s to be collected instead of the 10 s required for all the other type 2 PPIs.

Figure 3-3 represents this type 2 PPI scan collected north of the release pad, each spanning 30.0°. Figure 3-3 is a zoomed portion of the collected scan, covering an area of 1200 m × 930 m north of the release point. The bottom of the frame has two white blocks representing hard targets intercepted on the release pad. The bottom hard target was located at 3100 m from the REVEAL-Prototype.

Three faint plumes emerging from the bottom of the frame at locations –2700 m, –2950 m, and –3100 m are discernable. They all flow towards the north consistent with a wind direction of 145° from north.

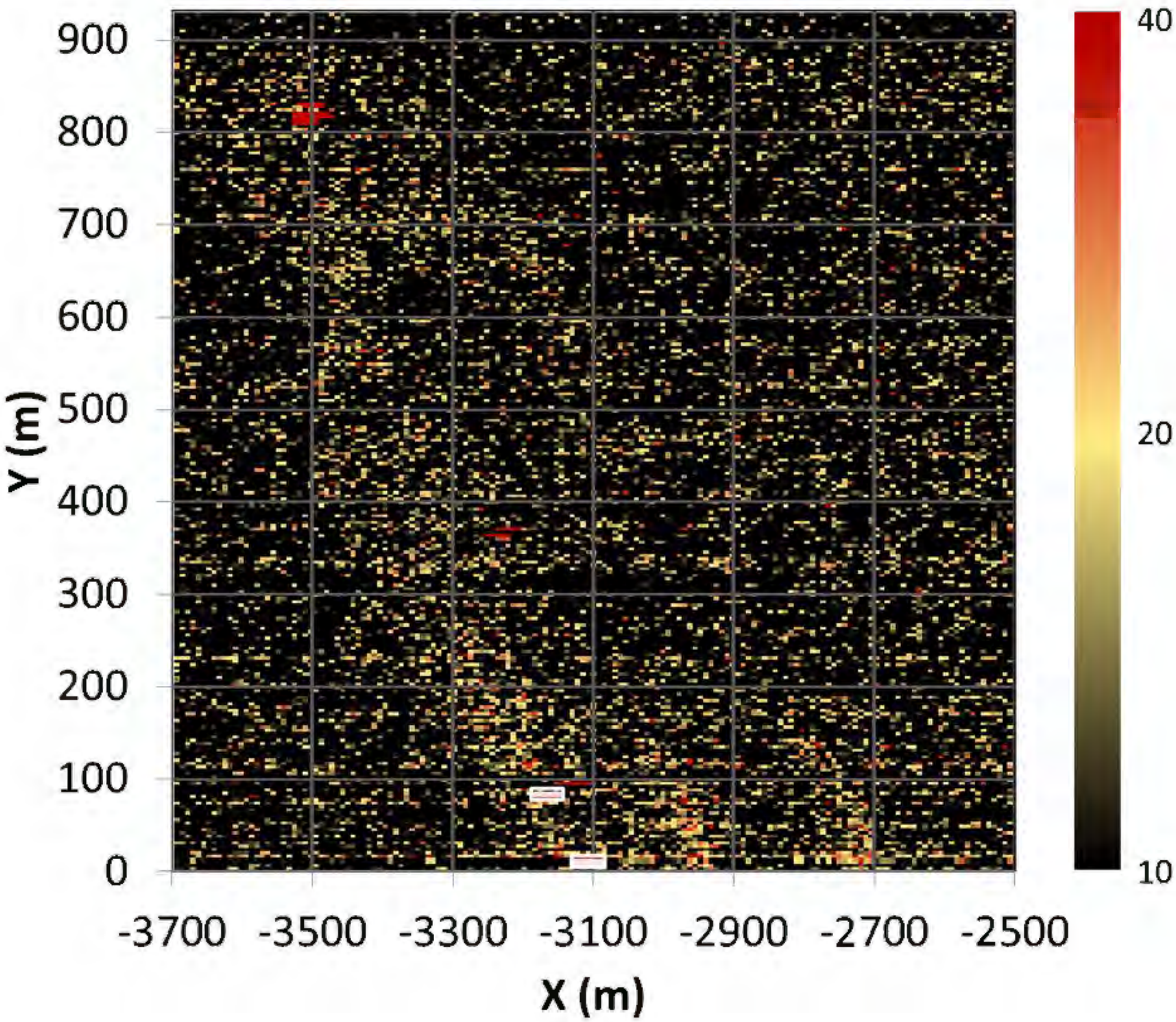

Figure 3-3. PPI scan type 2 collected at 14:28:21 UTC, JRII-6 test, directly north of the release point showing three plumes emerging from the release pad location. The two white blocks at the bottom are hard targets present on the release pad.

The remaining type 2 PPIs (Figure 3-4) did not visualize the Cl_2 aerosol cloud. It is not known if this is due to the nature of the aerosols still present in the cloud or if this is due to the improper setting of the elevation angle to optimally intercept the cloud.

In Figure 3-4, the plumes seen on the bottom of each vignette are due to the dust created by a vehicle driving on the dirt road towards the CP.

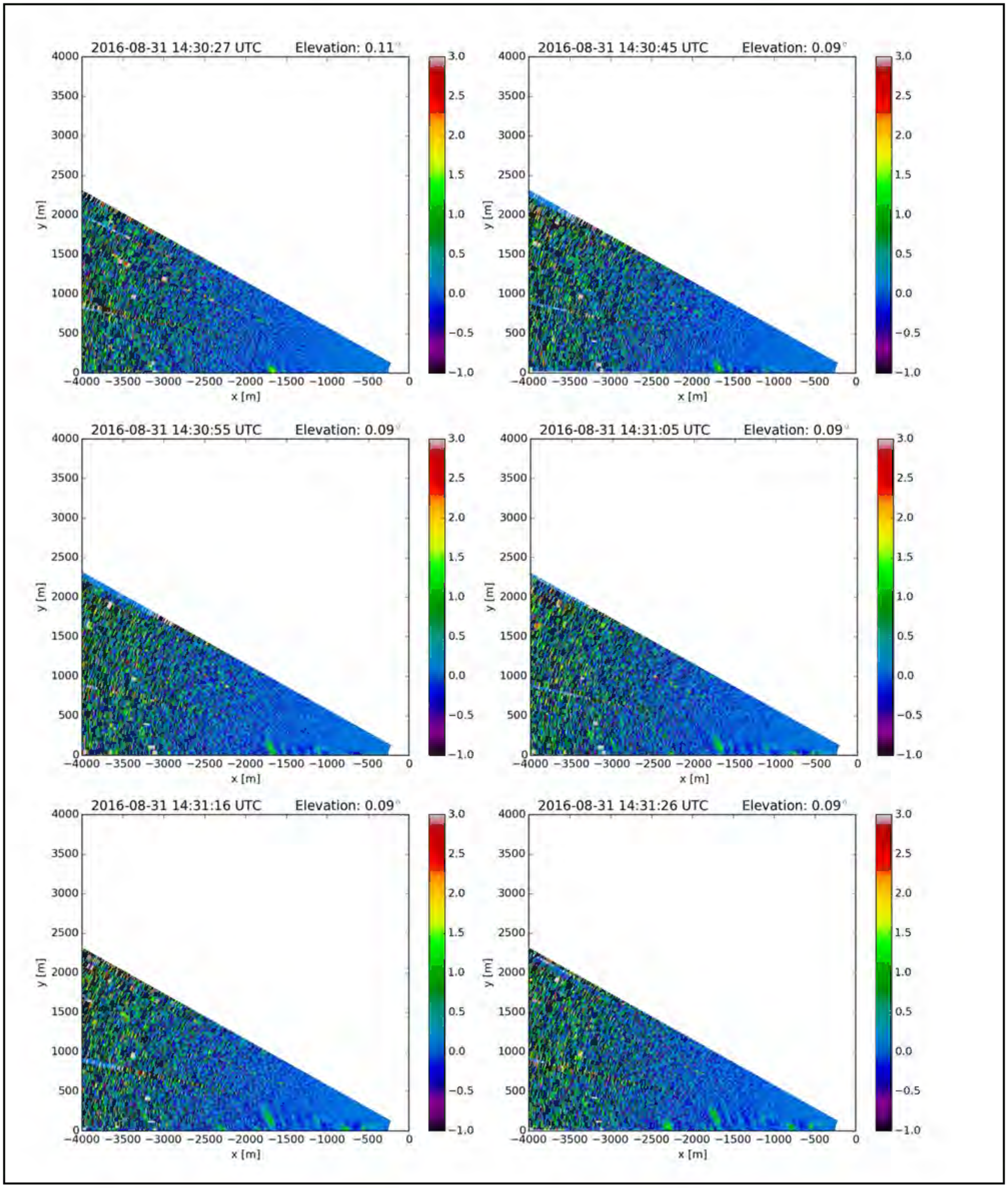

Figure 3-4. PPI scan type 2 collected during JRII-6 test, directly north of the release point

3.2 JRII-7 Test

Table 3-2. JRII-7 REVEAL configuration quick look summary

Parameter	Value	
Date	2 Sep 2016	
Release start (local time)	07:56:00	
Release stop (local time)	07:57:20	
Released Cl_2 weight (lb)	19,989	
Release orientation from vertical (°)	135	
Wind direction (°)	160	
Wind speed (m/s)	4.54	
REVEAL-Prototype status	On site / collecting data	
REVEAL-Prototype scan pattern	PPI scan type 1 at 0.12° elevation	
	Start time	07:30:00
	Stop time	08:11:58
	Start angle	268.28°
	Stop angle	270.26°
	Angular speed	0.0943°/s
REVEAL-5000 status	On site / no data collected	

3.2.1 PPI Type 1 Scans

For the first 15 min of this test, REVEAL-Prototype collected type 1 PPIs every 22.5 s (Figure 3-5) using a much slower scan speed than before.

Figure 3-5 is composed of six vignettes representing PPI scans collected over the release pad, each spanning 1.98°. This represents a south–north measured sweep length of 105 m at a range of 3050 m from the REVEAL sensor. Each vignette is a zoomed portion of the collected scan, covering an area of 3000 m × 140 m north of the release point.

The start of the PPI collection time (UTC) is provided above each vignette. The sweep starts from the southernmost point and proceeds clockwise towards the northernmost point. This forward sweep is accomplished in 21.0 s.

The elevation of 0.12° represented a height above the ground around 3 m estimated from the touch down location of the laser beam. This is above the height of a standard freight container. In these vignettes the hard-target footprint of two of the video towers are visible. These are represented by the bottom two large white squares in each vignette.

The release of Cl_2 occurred at 13:56:00 UTC with a release direction of 135° from the vertical.

Here also, in all the vignettes a north/south plume in the middle of the zoomed area is visible. This is believed to be an aerosol plume generated by the wind blowing over the access road south of the release pad.

The two middle vignettes from Figure 3-5 show a plume that can be attributed to the Cl_2 release. This plume emerges on the lidar scan sweep at the northeast corner of the south tower and propagates towards the north in the subsequent vignette.

For image processing convenience, the two middle vignettes from Figure 3-5 were converted to RTIs in Figure 3-6, where the lidar returns are presented as a range versus azimuth angle. The transverse dimensional scale associated with the 3050 m range is given on the left Y axis for reference. The vignettes are plotted in a Log10 intensity color scale. The locations of the release point and the aerosol station are indicated with a green pixel. On the left side vignette of Figure 3-6 corresponding to collection times between 13:56:27 and 13:56:48 UTC, the peak concentration of an emerging plume is detected at a range of 3062 m and at an azimuth of 268.8°. This plume is believed to be related to the release. This corresponds to a point located at northing 4445660 and easting 288099. The right-side vignette of Figure 3-6 correspond to collection times between 13:56:50 and 13:57:11 UTC. The observed aerosol plume edge, believed to be related to the release, intercepts the aerosol station and should be detected by that point sensor.

The plume relative concentration distribution found in the first frame (left side plot of Figure 3-6) has a close resemblance to the southern-edge plume distribution found on the second frame (right side plot of Figure 3-6). These two features are identified by the two white circles. The measured travel distance of this feature between the two frames is 13 m, corresponding to a ground velocity of 0.6 m/s. This is significantly below the anemometer-measured wind speed of 4.54 m/s. Tracking the aerosol features between frames to derive a ground speed might not be accurate in this particular case because the plume is lofting as it intercepts the lidar PPI plane. The plume boundaries are therefore expanding in all directions preventing a high confidence track of specific edge features. Further analysis correlating these lidar frames to videos might provide further insight.

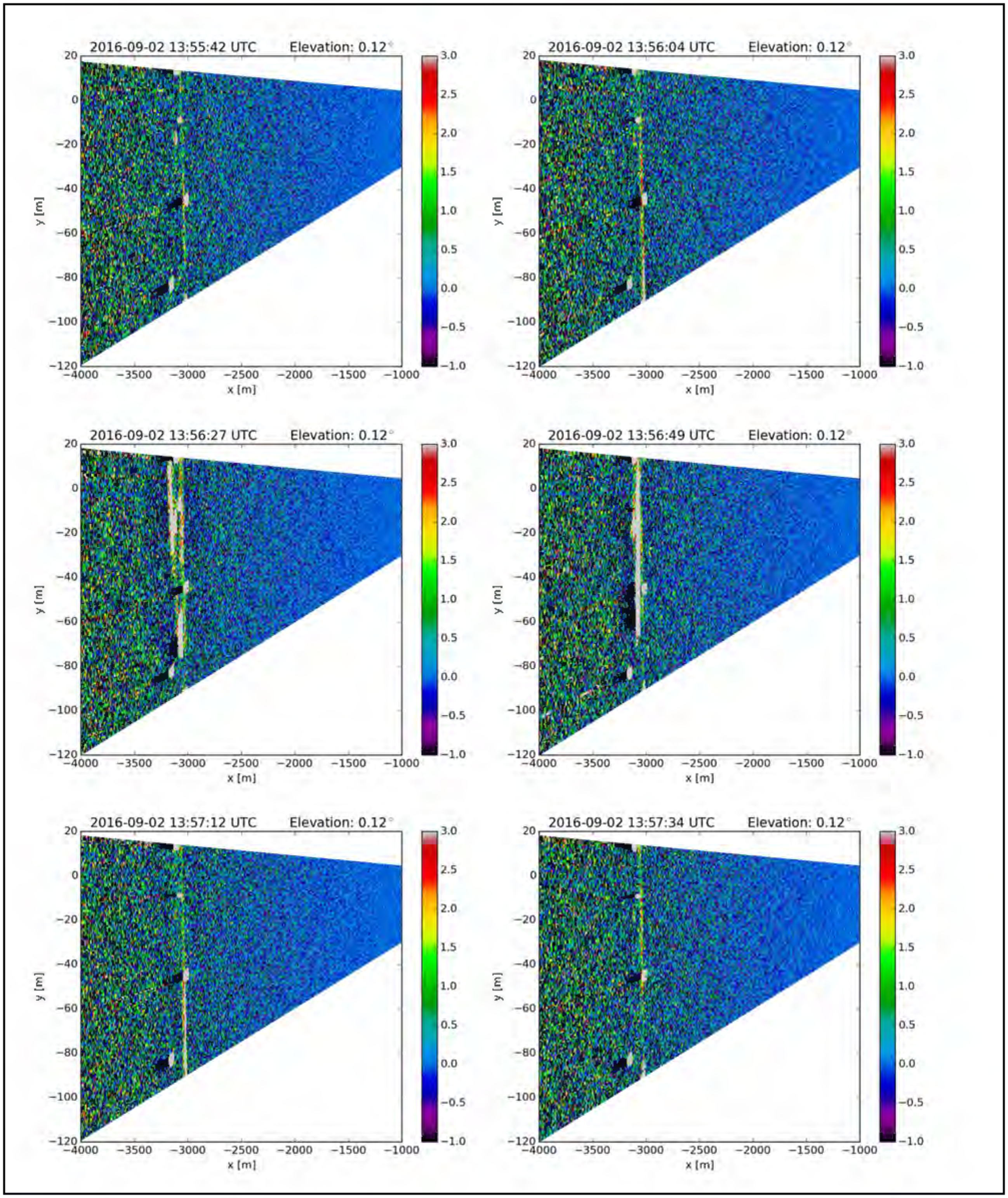

Figure 3-5. PPI scans above the release pad during the JRII-7 test. UTC time on top of each graph is start time of the scan; stop time of the scan is 21 s later.

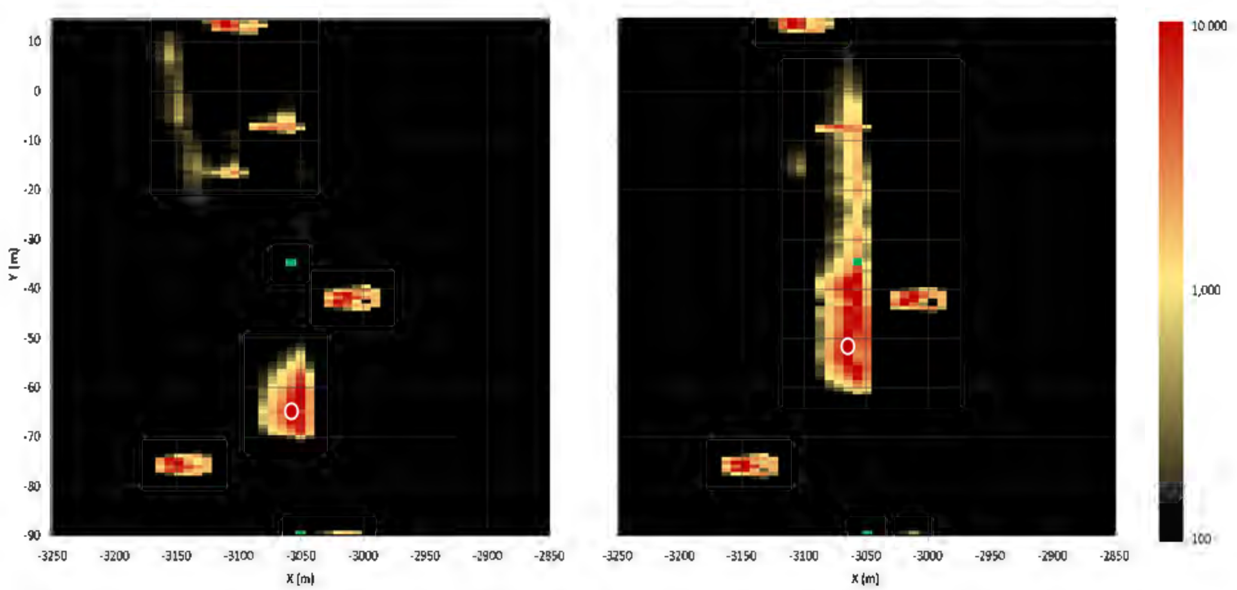

Figure 3-6. The two middle vignettes from Figure 3-5 (JRII-7) converted to RTI plots, in Log10 intensity scales. The left side RTI was measured during times 13:56:27 and 13:56:48, while the right side RTI was measured during times 13:56:50 and 13:57:11. The units of the intensity scales are proportional to photo counts backscattered from a given voxel. The release point and the aerosol station are indicated by green pixels at coordinates (–3052, –90) and (–3065, –36), respectively. On the right vignette, the aerosol plume intercepts the aerosol station (see Appendix A: Aerosol Arrival and Departure Time Analysis Using REVEAL Data for revised arrival time).

3.3 JRII-8 Test

Table 3-3. JRII-8 REVEAL configuration quick look summary

Parameter	Value	
Date	11 Sep 2016	
Release start (local time)	09:01:45	
Release stop (local time)	09:04:42	
Released Cl_2 weight (lb)	20,020	
Release orientation from vertical (°)	0	
Wind direction (°)	175	
Wind speed (m/s)	2.18	
REVEAL-Prototype status	On site / collecting data	
REVEAL-Prototype scan pattern	PPI scan type 1 at 0.11° elevation	
	Start time	08:50:51
	Stop time	09:04:31
	Start angle	268.29°
	Stop angle	270.26°
	Angular speed	0.222°/s
	PPI scan type 2 at 0.10° elevation	
	Start time	09:04:51
	Stop time	09:43:12
	Start angle	268.27°
	Stop angle	290.27°
	Angular speed	2°/s
REVEAL-5000 status	On site / collecting data	
REVEAL-5000 scan pattern	RHI at 268.30° azimuth	
	Start time	08:30:00
	Stop time	09:16:00
	Start angle	0.105°
	Stop angle	0.995°
	Angular speed	0.083°/s

3.3.1 PPI Type 1 Scans

For the first 2.75 min of this test, REVEAL-Prototype collected type 1 PPIs every 10.35 s (Figure 3-7, Figure 3-8, and Figure 3-9).

Figure 3-7 to Figure 3-9 are each composed of six vignettes representing PPI scans collected over the release pad, each spanning 1.97°. This represents a south–north measured sweep length of 105 m at a range of 3050 m from the REVEAL sensor. Each vignette is a zoomed portion of the collected scan, covering an area of 3000 m × 140 m north of the release point.

The start of the PPI collection time (UTC) is provided above each vignette. The sweep starts from the southernmost point and proceeds clockwise towards the northernmost point. This forward sweep is accomplished in 8.7 s.

The elevation of 0.11° represented a height above the ground around 2.5 m estimated from the touch down location of the laser beam. This is close to the height of a standard freight container. In these vignettes the hard-target footprint of two of the towers are visible. These are represented by the bottom two large white squares in each vignette.

The release of Cl_2 occurred at 15:01:45 UTC with a release direction of 0° from the vertical (straight up).

In all the vignettes there are north/south plumes between the ranges of 1000 and 3000 m in the zoomed area that are clearly visible. These were aerosol plumes generated by the wind blowing over the access road south of the release pad after the passing of a truck just before the release.

The bottom right vignette from Figure 3-7, all the vignettes from Figure 3-8, and the first three vignettes of Figure 3-9 show a plume that can be attributed to the Cl_2 release. This plume enters the lidar scan sweep at the west side of the northeast tower and propagates towards the north in all the subsequent vignettes.

Further analysis of these frames is presented in section 3.3.4 (Analysis 1 – Plume Touch Down Location).

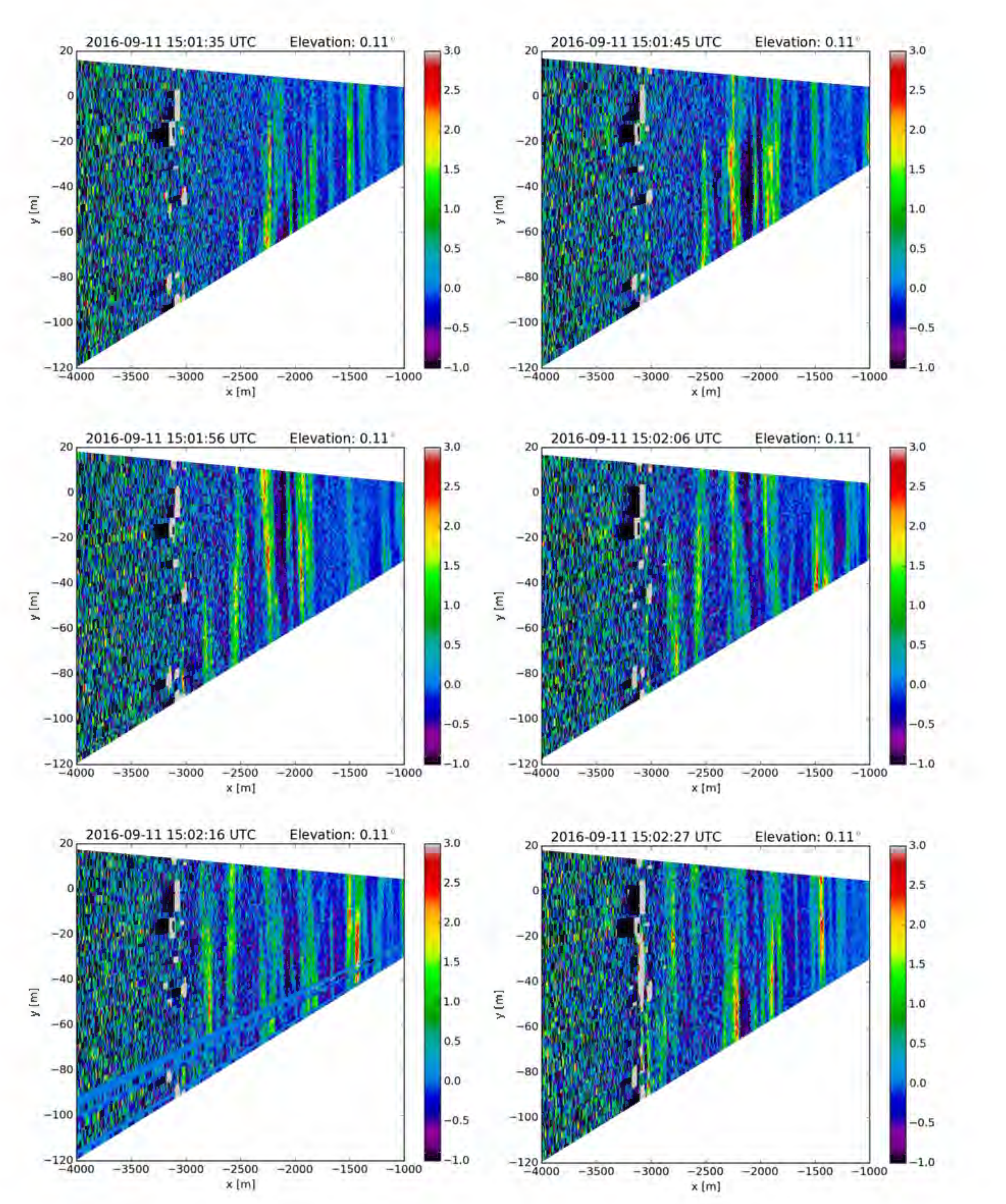

Figure 3-7. PPI scans above the release pad during the JRII-8 test. UTC time on top of each graph is start time of the scan; stop time of the scan is 8.7 s later.

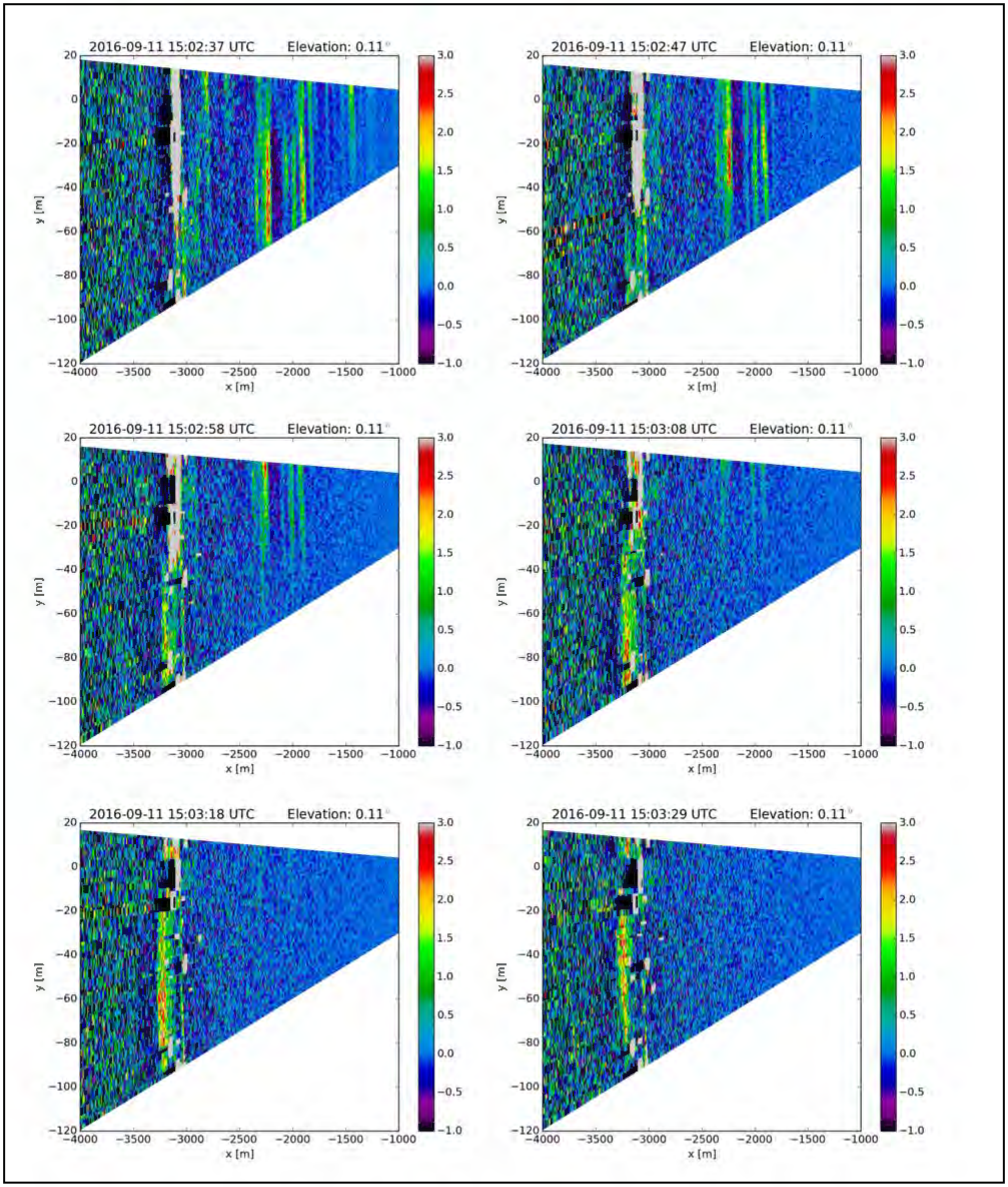

Figure 3-8. PPI scans above the release pad during the JRII-8 test. UTC time on top of each graph is start time of the scan; stop time of the scan is 8.7 s later.

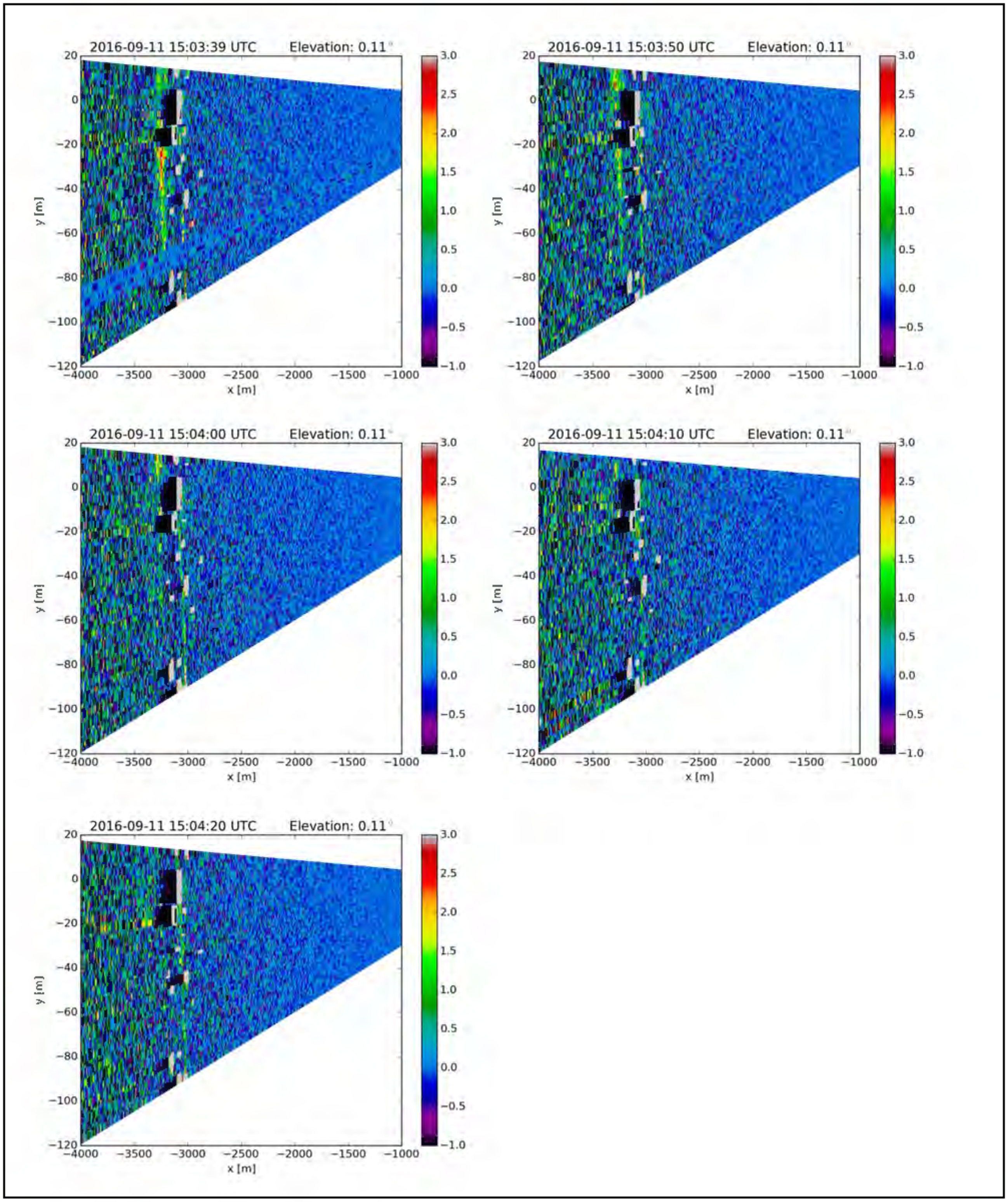

Figure 3-9. PPI scans above the release pad during the JRII-8 test. UTC time on top of each graph is start time of the scan; stop time of the scan is 8.7 s later.

3.3.2 PPI Type 2 Scans

After the PPI type 1 scans and for the following 6 min of this test, REVEAL-Prototype collected type 2 PPIs every 13.5 s (Figure 3-10, Figure 3-11, and Figure 3-12).

Figure 3-10 to Figure 3-12 are each composed of six vignettes representing PPI scans collected over the release pad and north of the release pad, each spanning 22°. This represents a south–north measured sweep length of 1232 m at a range of 3050 m from the REVEAL sensor. Each vignette is a zoomed portion of the collected scan, covering an area of 3000 m × 1600 m north of the release point.

The start of the PPI collection time (UTC) is provided above each vignette. The sweep starts from the southernmost point and proceeds clockwise towards the northernmost point. This forward sweep is accomplished in 11.5 s.

In each of the graphs, a southwest to northeast line of plumes propagates from the south portion of each PPI towards the north. The westernmost plume is the one that emerged from the release pad, the others being the leftover dust plume from a truck travelling towards the CP on the dirt road.

In each of the graphs, a cluster of white pixels is observed on the southern part of the scan at range –3000 to –3400 m. These correspond to the hard targets intercepted on the release pad and north of the release pad. Between Y = –120 m and Y = 0 m, these are the same hard targets observed in PPI type 1 scans that have been compressed in the Y dimension due to the re-scaling effect.

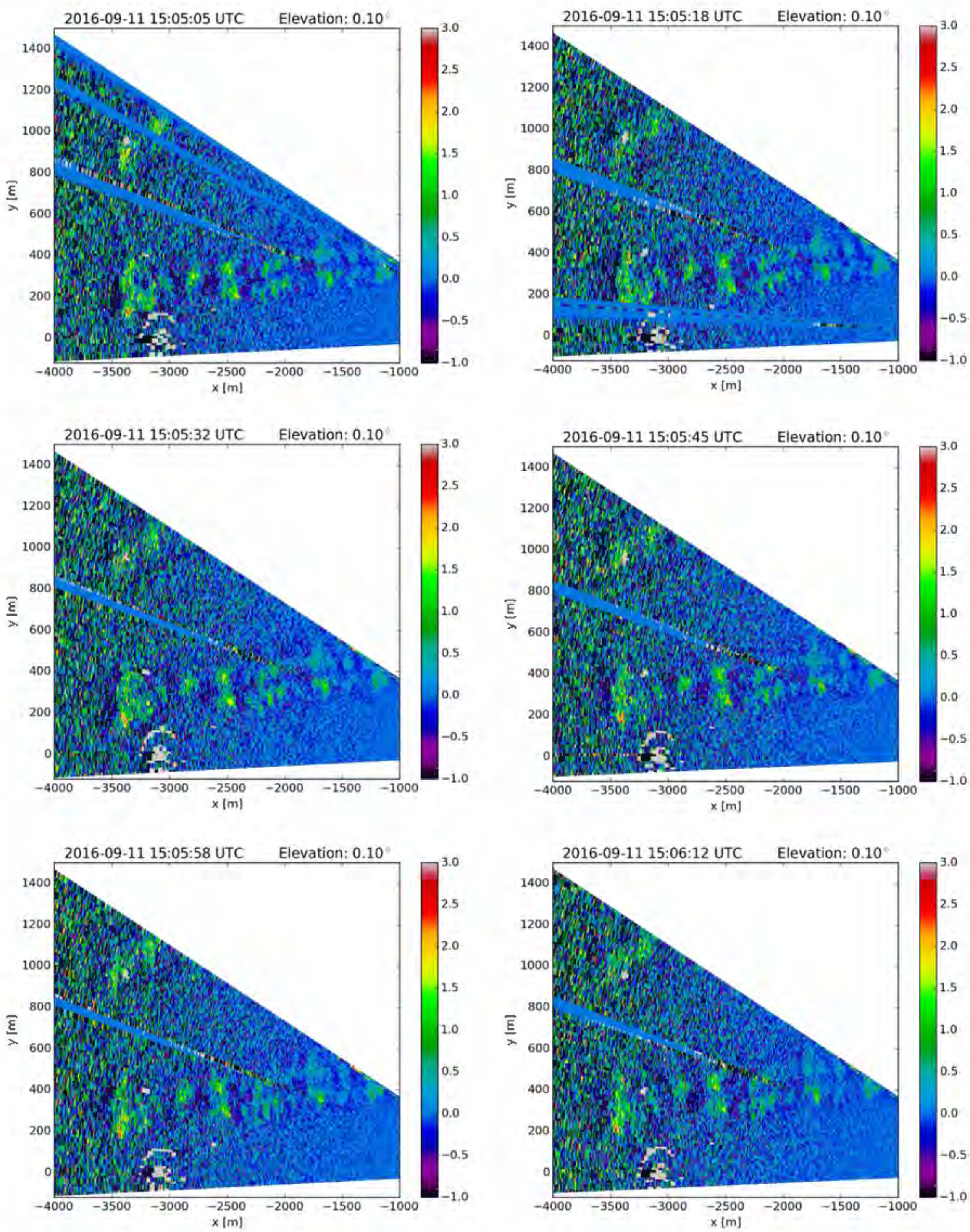

Figure 3-10. PPI scans north of the release pad during the JRII-8 test. UTC time on top of each graph is start time of the scan; stop time of the scan is 12 s later.

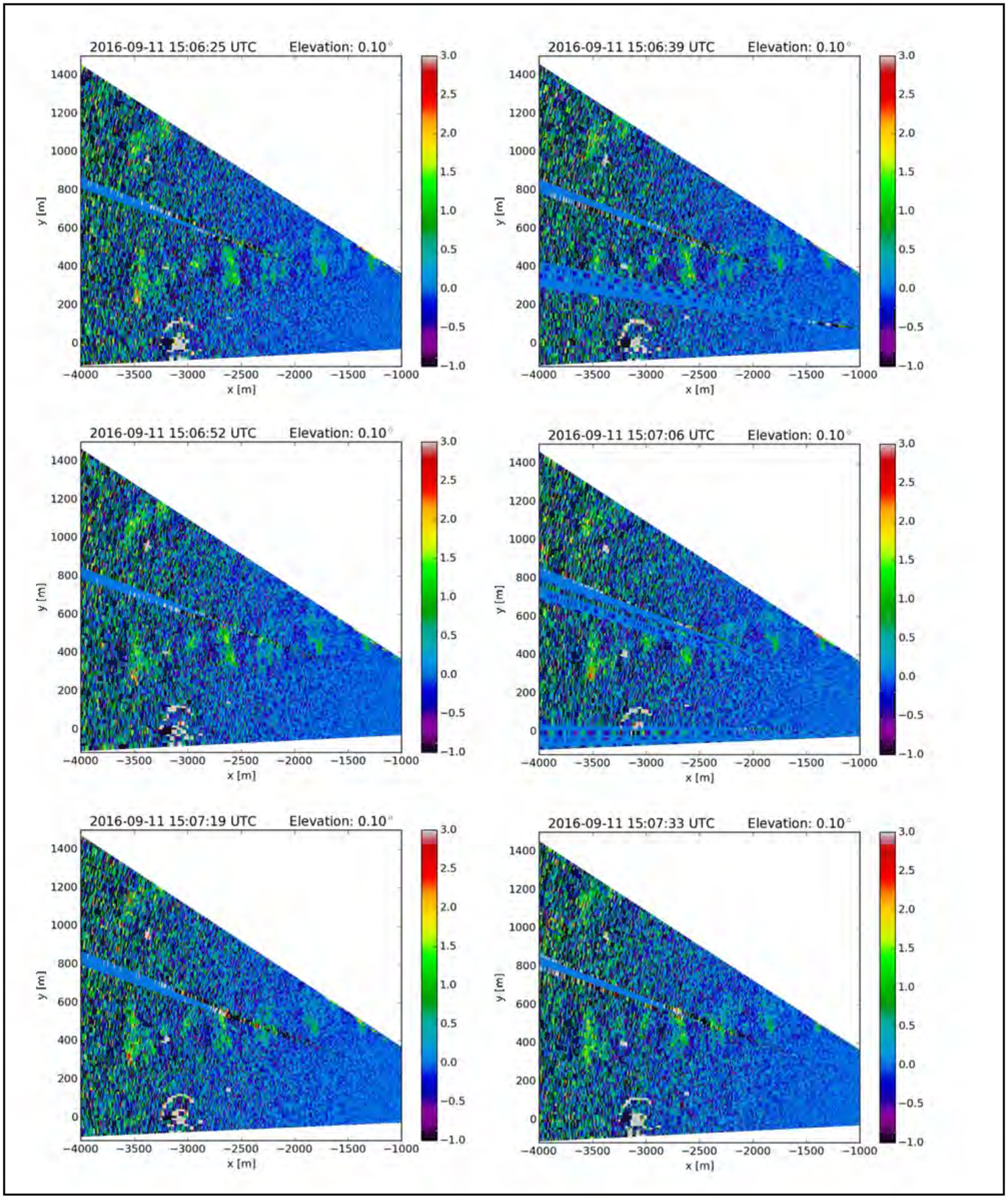

Figure 3-11. PPI scans north of the release pad during the JRII-8 test. UTC time on top of each graph is start time of the scan; stop time of the scan is 12 s later.

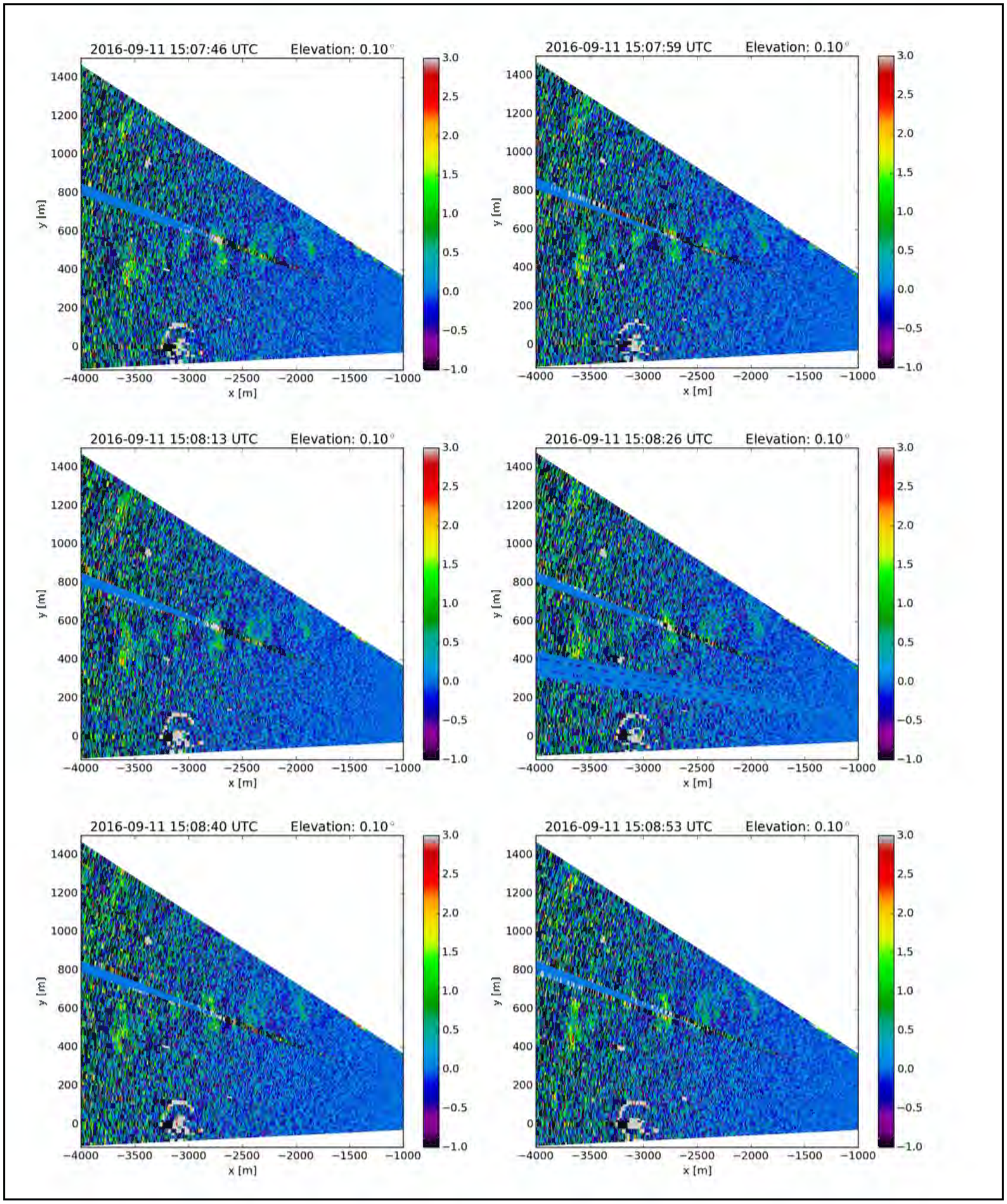

Figure 3-12. PPI scans north of the release pad during the JRII-8 test. UTC time on top of each graph is start time of the scan; stop time of the scan is 12 s later.

3.3.3 RHI Scans

For the first 15 min of this test, REVEAL-5000 collected RHIs every 17.5 s (Figure 3-13).

Figure 3-13 is composed of four vignettes representing RHI scans collected over the release point, each spanning 0.88° in elevation. This represents a bottom to top measured sweep height of 47.8 m at a range of 3044 m from the REVEAL sensor. Each vignette is a zoomed portion of the collected scan, covering an area of 2500 m × 80 m in the vertical plane above the release point.

The start of the RHI collection time (UTC) is provided above each vignette. The sweep starts from the bottom point and proceeds upwards towards the top point. This forward sweep is accomplished in 10.6 s. The fly-back sweep is accomplished in 6.6 s.

The azimuth angle of the elevation sweeps was set at 268.30° representing the direction of the tank (the graphs in Figure 3-16 have an uncorrected azimuth pointing direction of 261.54°). The starting elevation angle of each sweep is 0.105° and corresponds to the top of the Cl_2 tank.

Further analysis of these frames is presented in section 3.3.5 (Analysis 2 – Plume Vertical Distribution and Maximum Height).

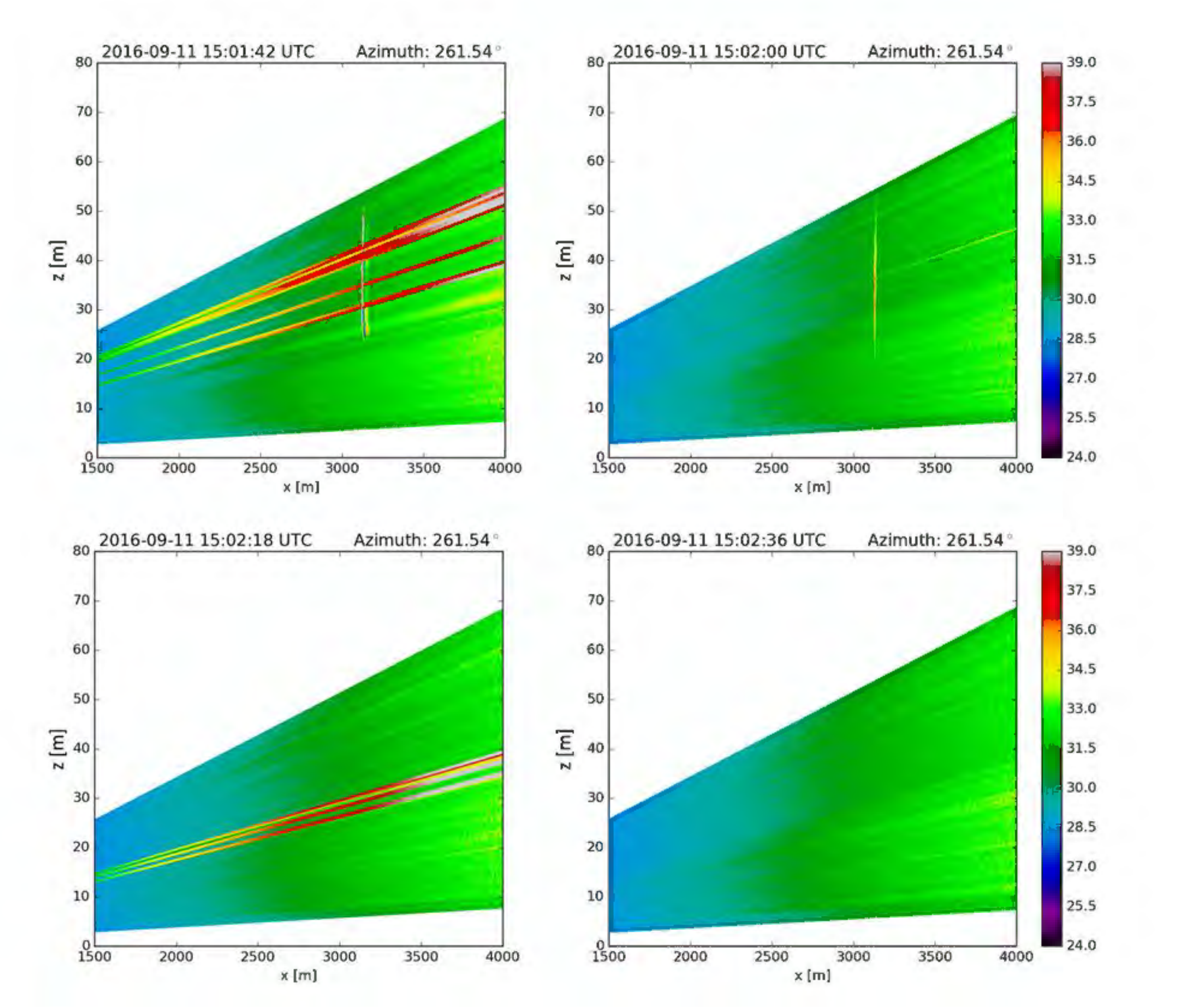

Figure 3-13. RHI scans collected by the REVEAL-5000 during JRII-8 test, directly above the Cl_2 tank while the REVEAL-Prototype was collecting PPI type 1 scans

3.3.4 Analysis 1 – Plume Touch Down Location

In order to precisely identify the dense plume touch down location after the vertical ejection of the gas and aerosols and the following dense plume slumping to ground, we analyzed a subset of PPI type 1 scans collected with the REVEAL-Prototype.

To facilitate image processing and for presentation clarity, the PPI images shown in Figure 3-7, Figure 3-8, and Figure 3-9 were converted to filtered RTI images covering only a 468 m × 105 m area above the release pad (Figure 3-15 to Figure 3-21). The strong signals associated with the hard target were also eliminated by subtracting exclusion zones. This reduces the hard-target interferences when visualizing and mapping the dense gas-aerosol plume as it intercepts the volume scanned by the system. For scale clarity, the locations of the release point and the aerosol station are also indicated in these RTIs with two white pixels. Figure 3-14 describes the data transformation that starts with the PPIs described in Figure 3-7 to Figure 3-9 and produces the RTIs shown in Figure 3-15 to Figure 3-21.

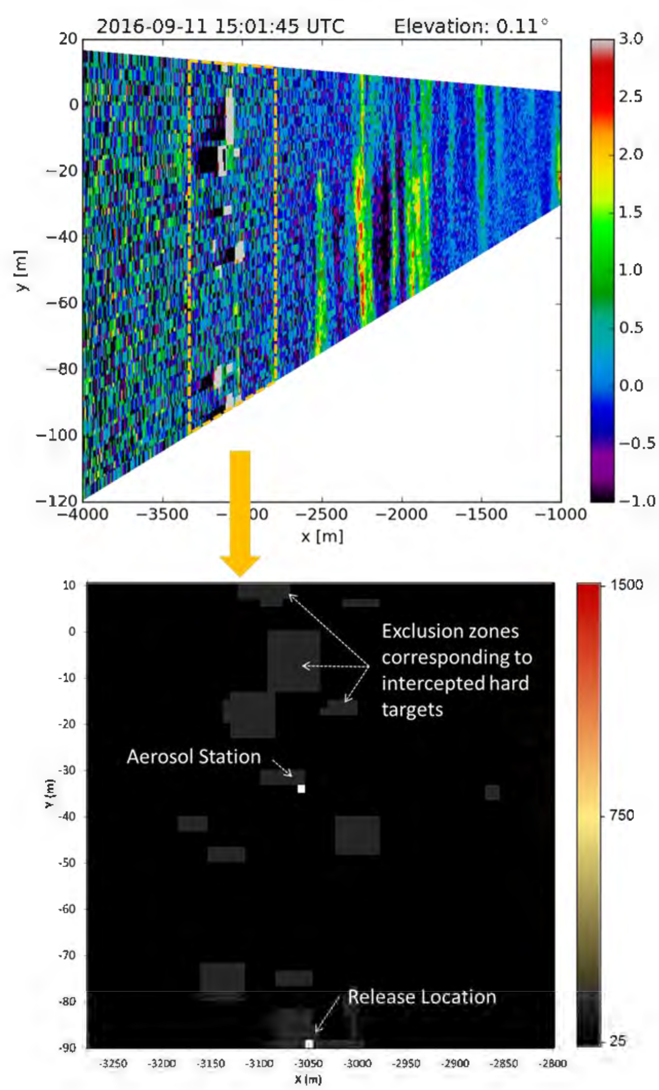

Figure 3-14. Data transform used to enhance the aerosol plume relative concentration visualization around the release point. The color scale on the right of the bottom graph corresponds to aerosol-backscattered photo counts collected in each voxel. The voxel size is 2.05 m × 7.7 m × 0.45 m.

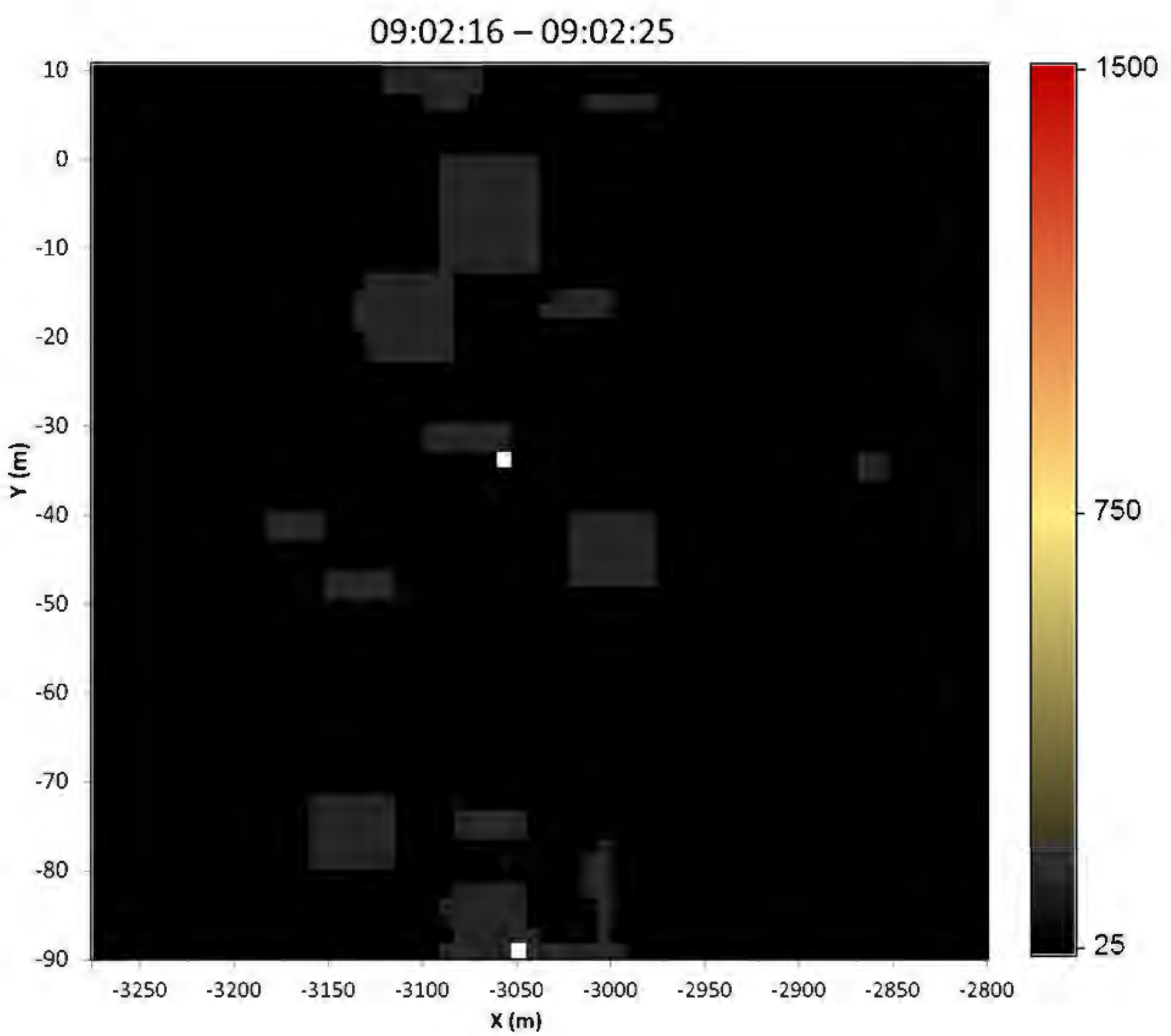

Figure 3-15. RTI plot of the aerosol distribution downwind from the release point (same frame as the lower left vignette of Figure 3-7, JRII-8). The time frame corresponding to this RTI is indicated at the top of the graph. The RTI was collected starting with low values of the Y dimension and build up towards higher values of Y as the sensor scans above the release pad. The height above ground of this RTI plot is around 3 m. This particular RTI is collected while the aerosol jet plume has not yet fallen down onto the release pad. It provides a map of clear conditions.

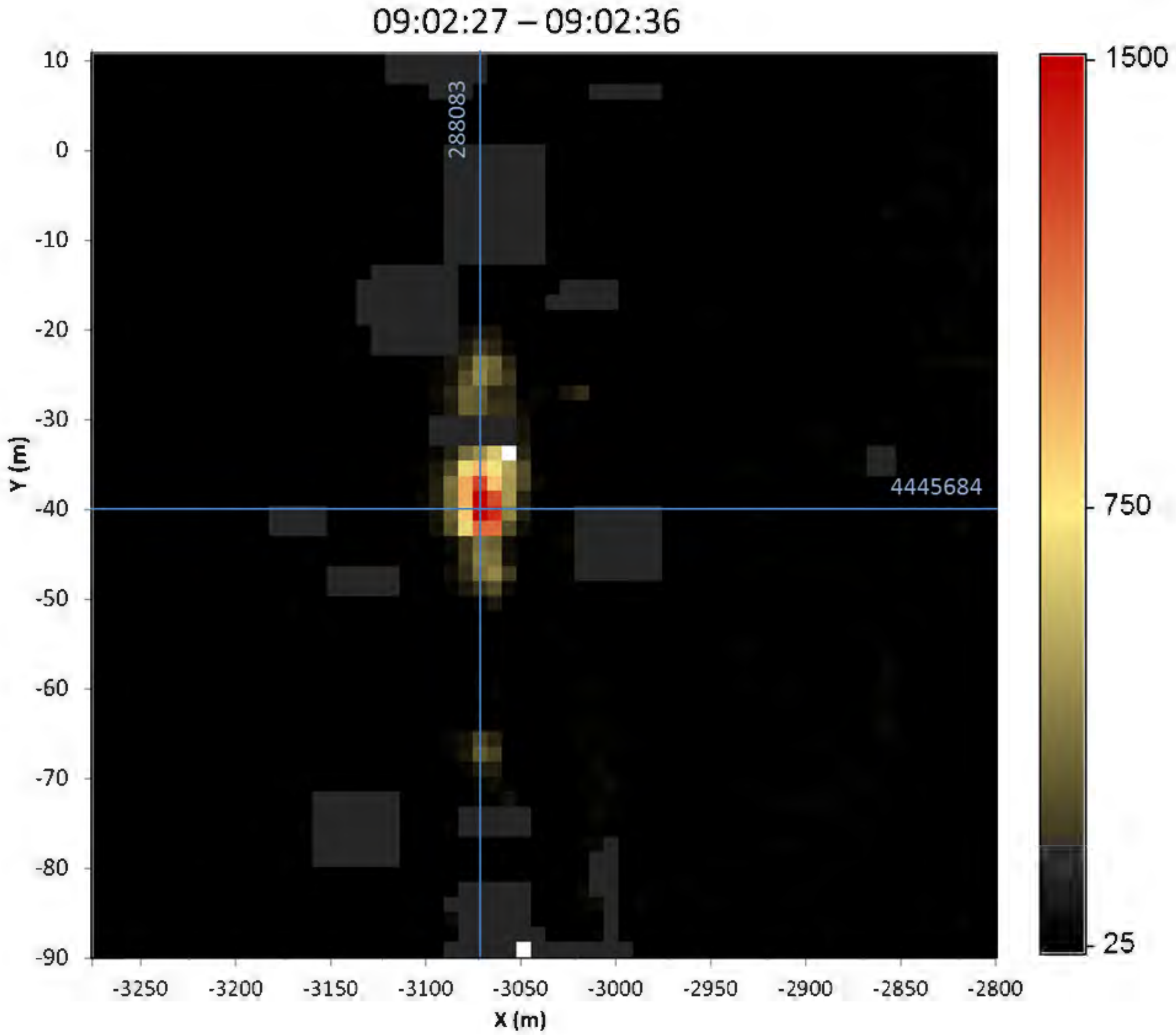

Figure 3-16. RTI plot of the aerosol distribution downwind from the release point (same frame as the lower right vignette of Figure 3-7, JRII-8). The time frame corresponding to this RTI is indicated at the top of the graph. The RTI was collected starting with low values of the Y dimension and build up towards higher values of Y as the sensor scans above the release pad. The height above ground of this RTI plot is around 3 m. This particular RTI is collected when the aerosol jet plume has just started falling down onto the release pad. This is the critical lidar scan that provides a map of touch down conditions. The corresponding UTM northing and easting of the peak concentration are 4445684 m and 288083 m, respectively. The aerosol station is intercepted by the aerosol cloud in this lidar frame (see Appendix A: Aerosol Arrival and Departure Time Analysis Using REVEAL Data for revised arrival time).

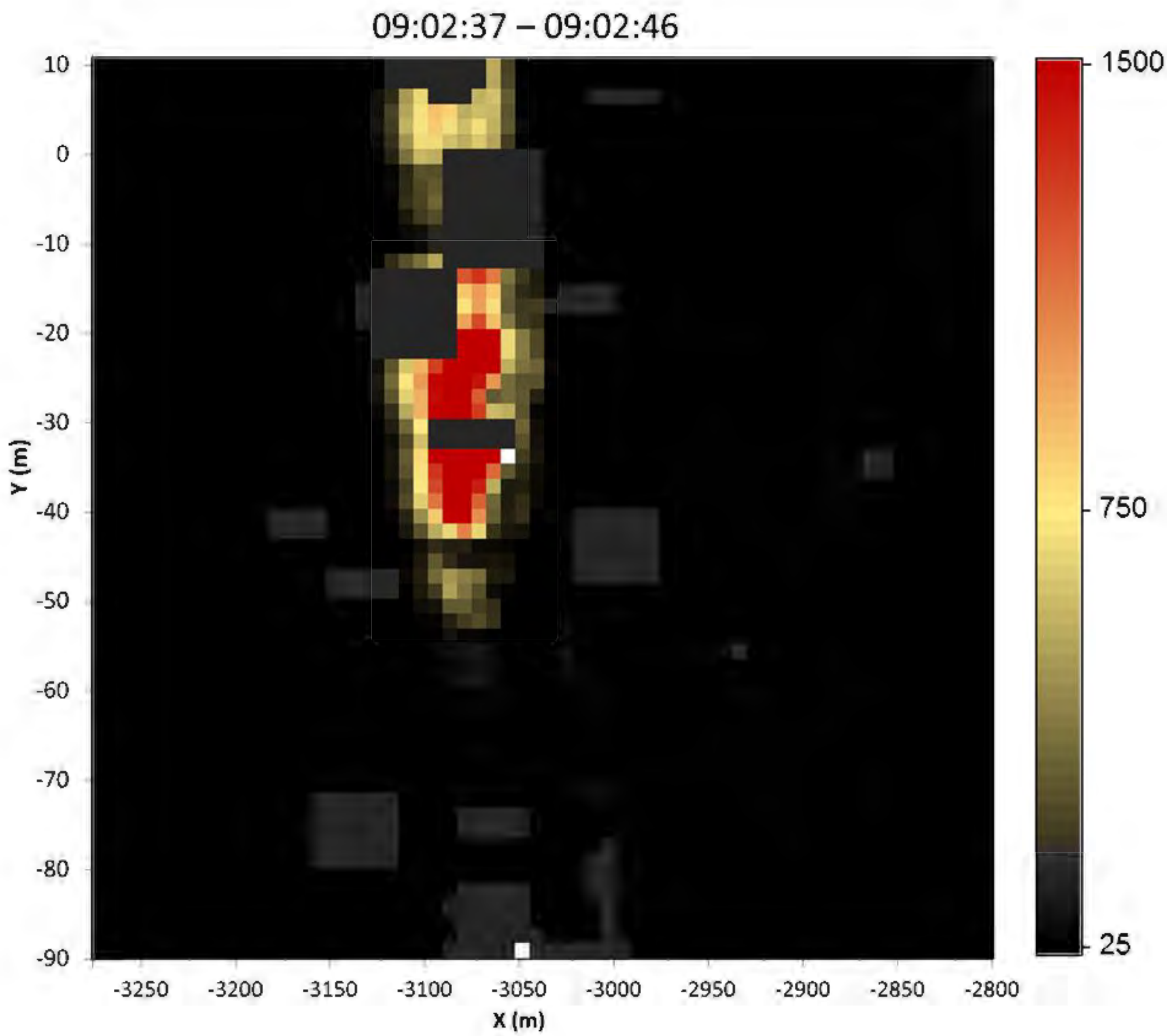

Figure 3-17. RTI plot of the aerosol distribution downwind from the release point (same frame as the top left vignette of Figure 3-8, JRII-8). The time frame corresponding to this RTI is indicated at the top of the graph. The RTI was collected starting with low values of the Y dimension and build up towards higher values of Y as the sensor scans above the release pad. The height above ground of this RTI plot is around 3 m. This particular RTI is collected when the aerosol jet plume has fallen down onto the release pad. It provides a map of the maximum relative concentration observed on the release pad 10.4 s after touch down. The aerosol station is intercepted by the aerosol cloud in this frame (see Appendix A: Aerosol Arrival and Departure Time Analysis Using REVEAL Data for revised arrival time).

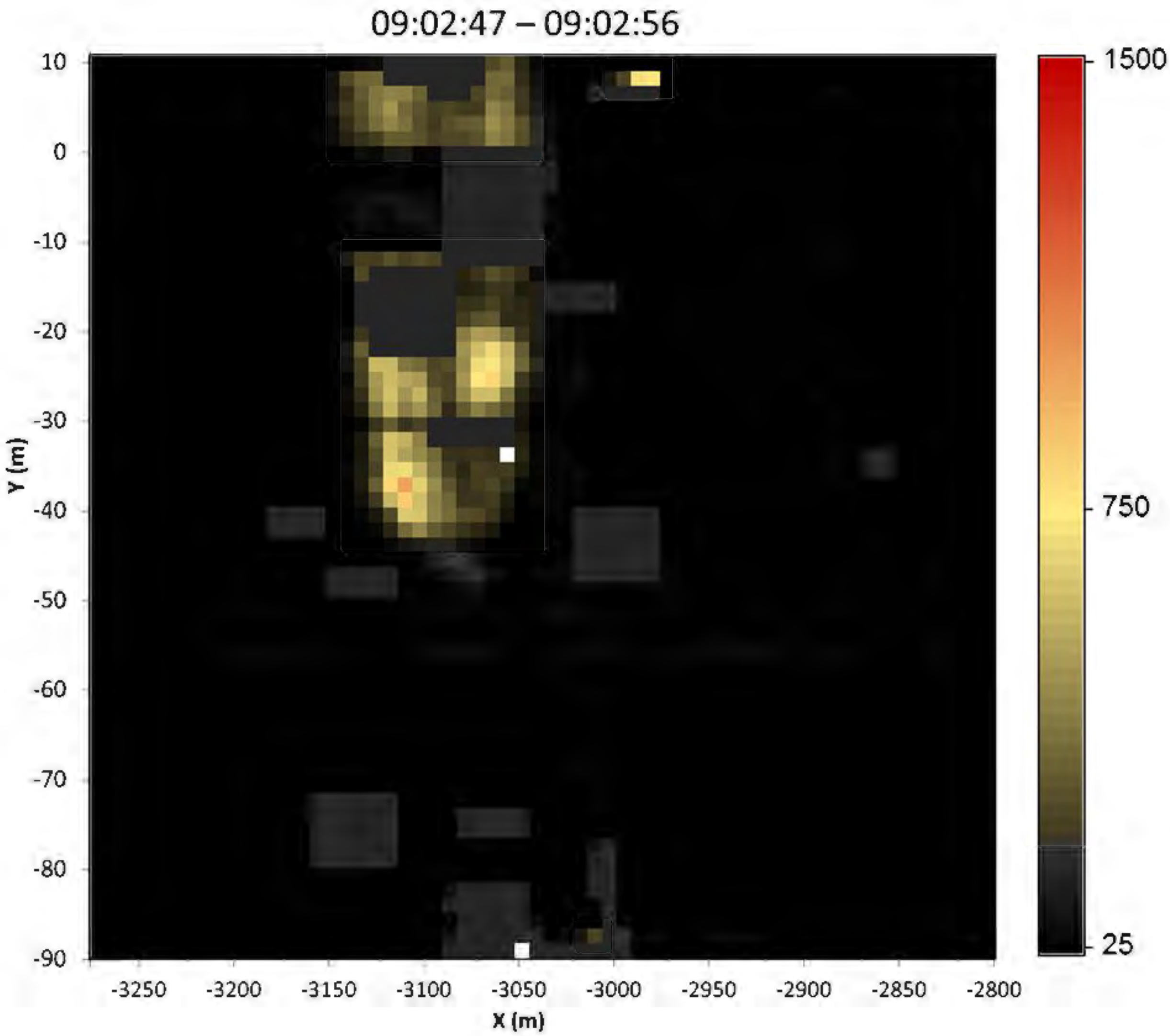

Figure 3-18. RTI plot of the aerosol distribution during JRII-8 test, downwind from the release point. The time frame corresponding to this RTI is indicated at the top of the graph. The RTI was collected starting with low values of the Y dimension and build up towards higher values of Y as the sensor scans above the release pad. The height above ground of this RTI plot is around 3 m. This particular RTI is collected when the aerosol jet plume has fallen down onto the release pad. It provides a map of relative aerosol concentration 20.8 s after touch down. The aerosol station is intercepted by the aerosol cloud in this frame (see Appendix A: Aerosol Arrival and Departure Time Analysis Using REVEAL Data for revised arrival time).

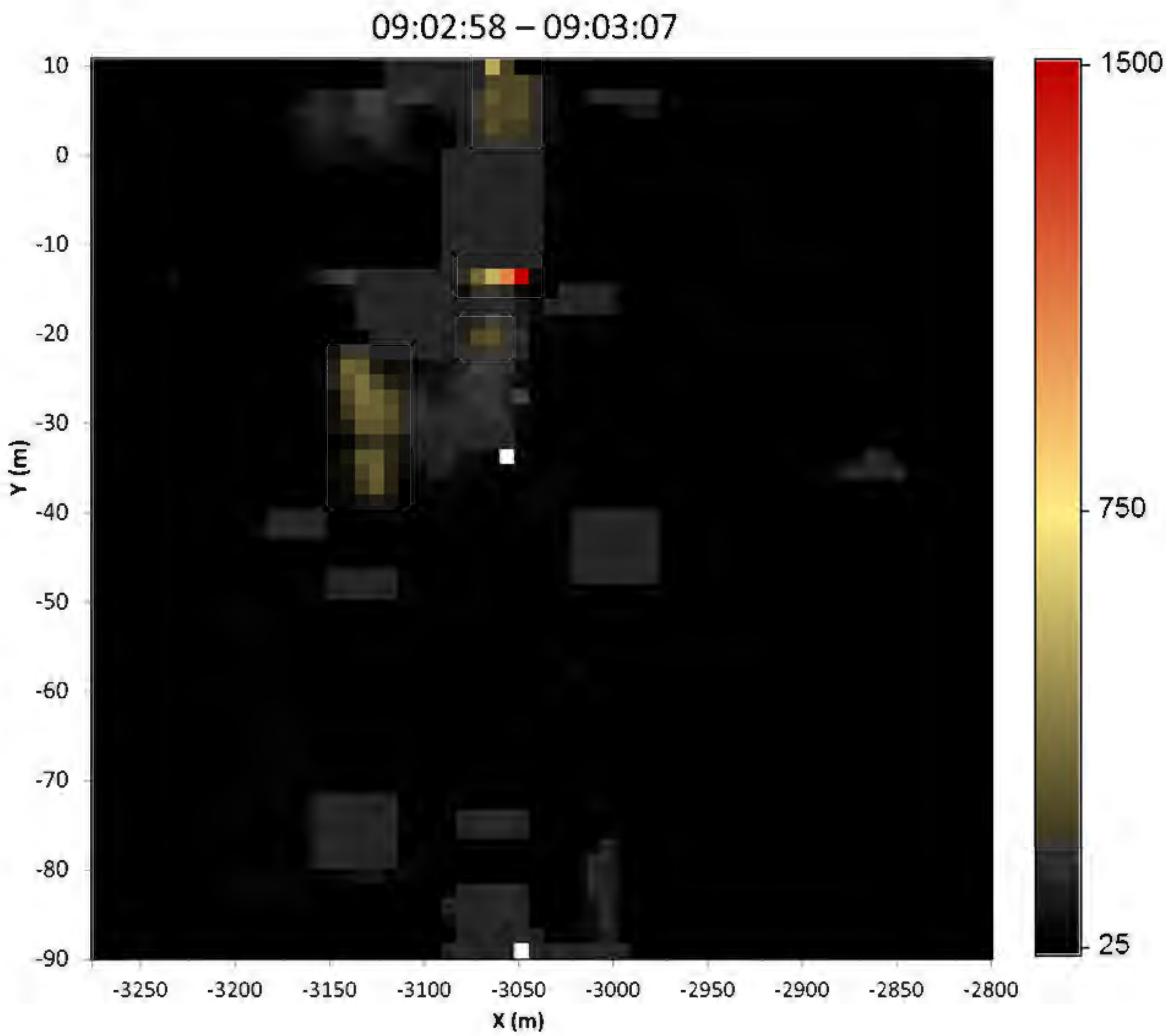

Figure 3-19. RTI plot of the aerosol distribution during JRII-8 test, downwind from the release point. The time frame corresponding to this RTI is indicated at the top of the graph. The RTI was collected starting with low values of the Y dimension and build up towards higher values of Y as the sensor scans above the release pad. The height above ground of this RTI plot is around 3 m. This particular RTI is collected when the aerosol jet plume has fallen down onto the release pad. It provides a map of relative aerosol concentration 31.4 s after touch down. The aerosol station is intercepted by the aerosol cloud in this frame (see Appendix A: Aerosol Arrival and Departure Time Analysis Using REVEAL Data for revised arrival time).

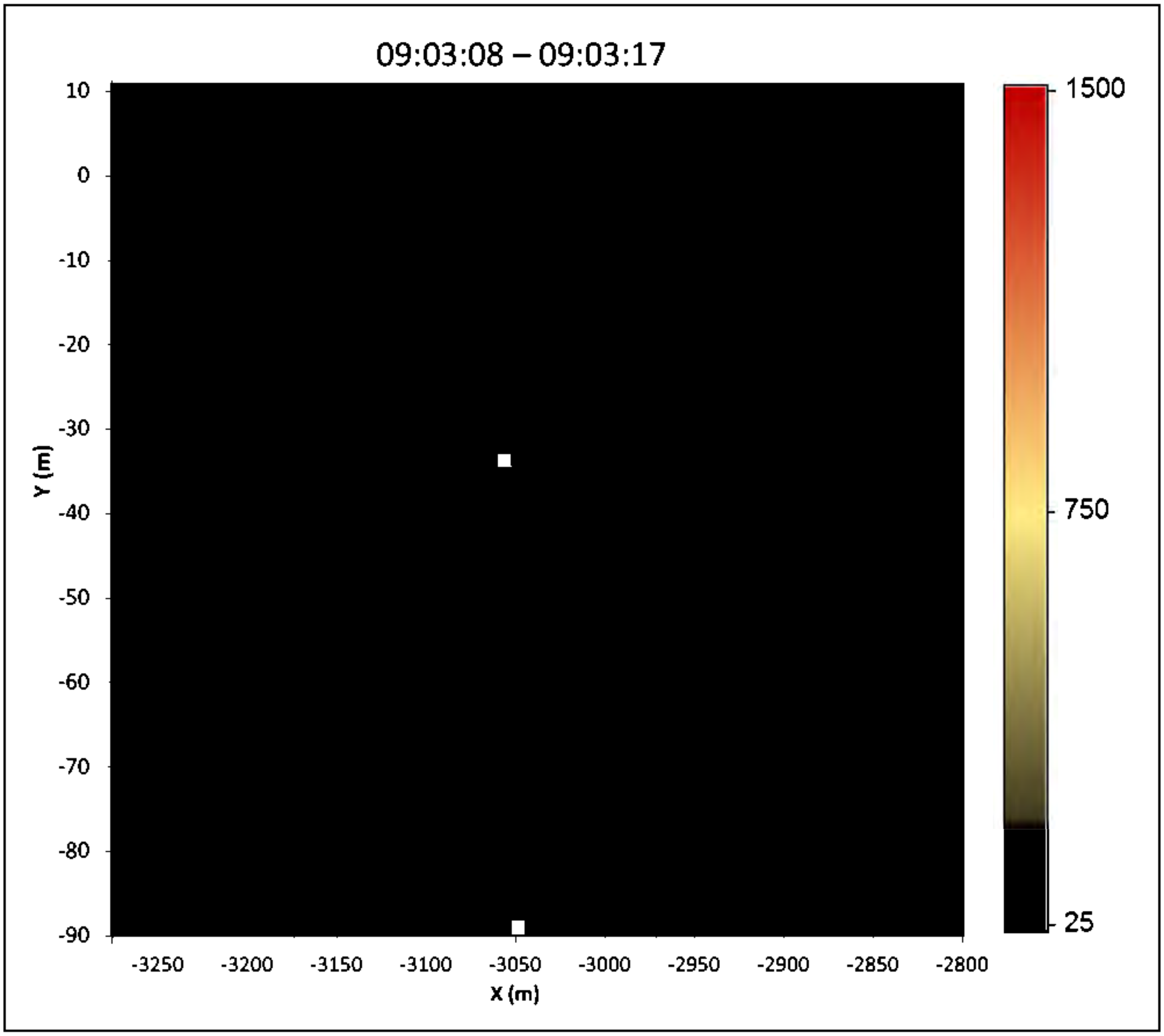

Figure 3-20. RTI plot of the aerosol distribution during JRII-8 test, downwind from the release point. The time frame corresponding to this RTI is indicated at the top of the graph. The RTI was collected starting with low values of the Y dimension and build up towards higher values of Y as the sensor scans above the release pad. The height above ground of this RTI plot is around 3 m. This particular RTI is collected when the aerosol jet plume has fallen down onto the release pad. It provides a map of relative aerosol concentration 41.7 s after touch down. Only aerosol clouds north of the aerosol station are detected by the lidar.

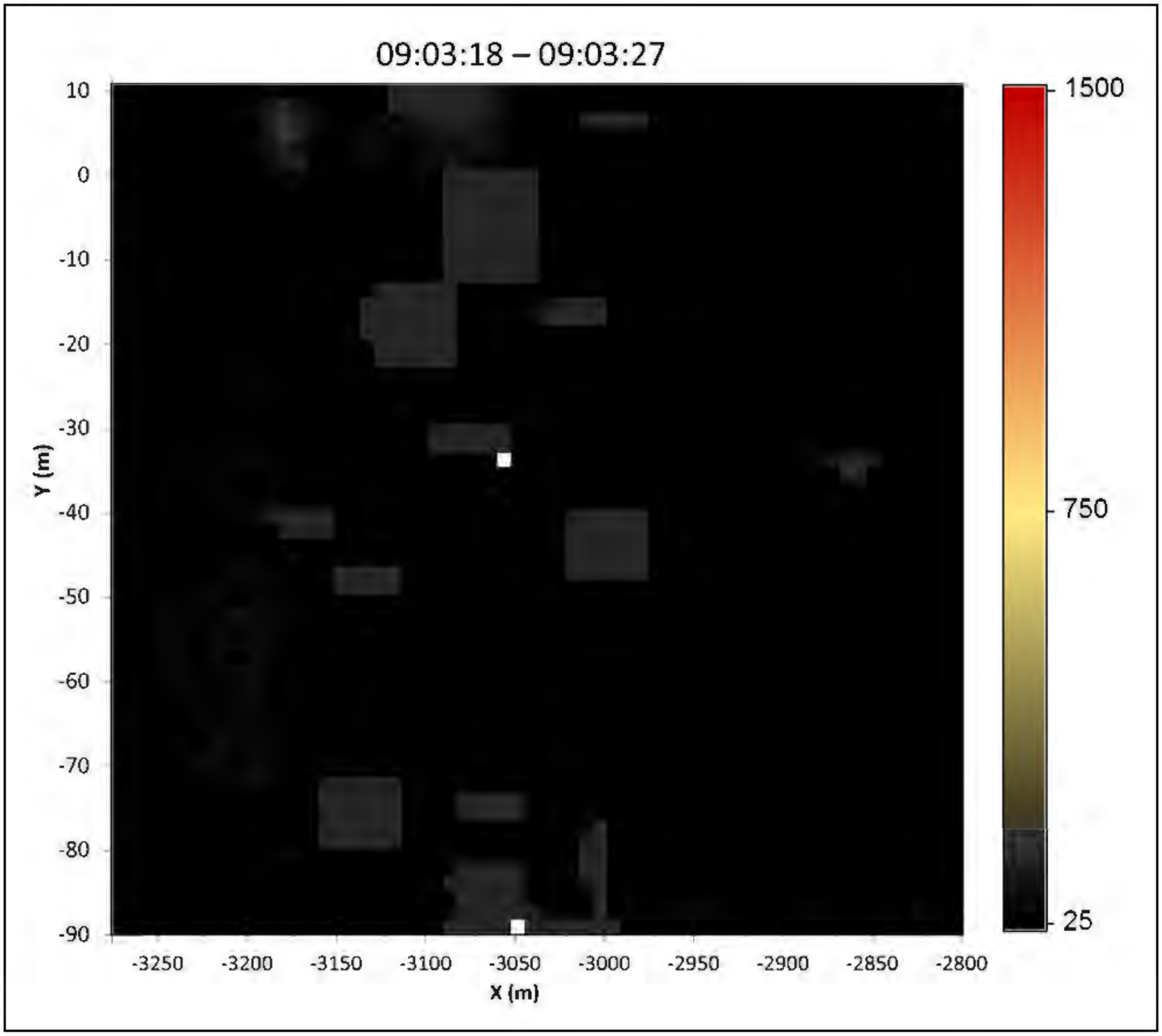

Figure 3-21. RTI plot of the aerosol distribution during JRII-8 test, downwind from the release point. The time frame corresponding to this RTI is indicated at the top of the graph. The RTI was collected starting with low values of the Y dimension and build up towards higher values of Y as the sensor scans above the release pad. The height above ground of this RTI plot is around 3 m. This particular RTI is collected when the aerosol jet plume has fallen down onto the release pad. It provides a map of relative aerosol concentration 52 s after touch down. Only aerosol clouds north of the aerosol station are detected by the lidar.

The selected PPI scan strategy worked very well in capturing the touch down conditions of the aerosol plume. At 09:02:32, the aerosol plume maximum relative concentration is intercepted by the lidar scan, providing the touch down location. The corresponding UTM northing and easting of the peak concentration are 4445684 m and 288083 m, respectively (Figure 3-16). The aerosol station was in the immediate vicinity and the aerosol cloud should have intercepted it.

3.3.5 Analysis 2 – Plume Vertical Distribution and Maximum Height

The REVEAL-5000 was configured to capture RHI scans in an effort to document the vertical distribution and maximum height of the aerosol plume emerging above the tank. For that reason, the line of sight of the scanner was positioned just above the release point. From these raw RHI scans (Figure 3-13), we used a data transformation process to extract the maximum information and better visualize the plume distribution and height. The resulting filtered RHI images are shown in Figure 3-22 to Figure 3-26. Since the scanner was setup for relatively low fly-back speeds, we did retrieve also the fly-back scans to extract associated RHIs. Since these were done at higher maximum speeds and scanner was rapidly decelerated, several corrections to the data needed to be made.

Each RHI provides a 155 m × 47 m area representing a relative aerosol concentration directly above the release point. The horizontal axis has been scaled in relative depth, with 0 m being the range location of the release point. The vertical axis has been scaled in relative elevation above the release point, 0 m being the height of the top of the tank.

Figure 3-22 provides the first sweep intercepting the vertical aerosol jet. Using REVEAL-5000 local clock, the sweep started at 15:01:43 UTC just before the release. As the laser beam scans up, the laser beam intercepts the aerosol jet at 15:01:47 when the laser is 17.8 m above the release point. Since the release time was made at 15:01:45 UTC (network time), we believe the REVEAL-5000 clock was 2 s ahead of the network time. Using REVEAL-5000 local clock, the laser beam stopped intercepting the aerosol jet at 15:01:53 when the laser beam was 44 m above the tank. The length of vertical aerosol jet intercepted by the lidar system is therefore 26 m.

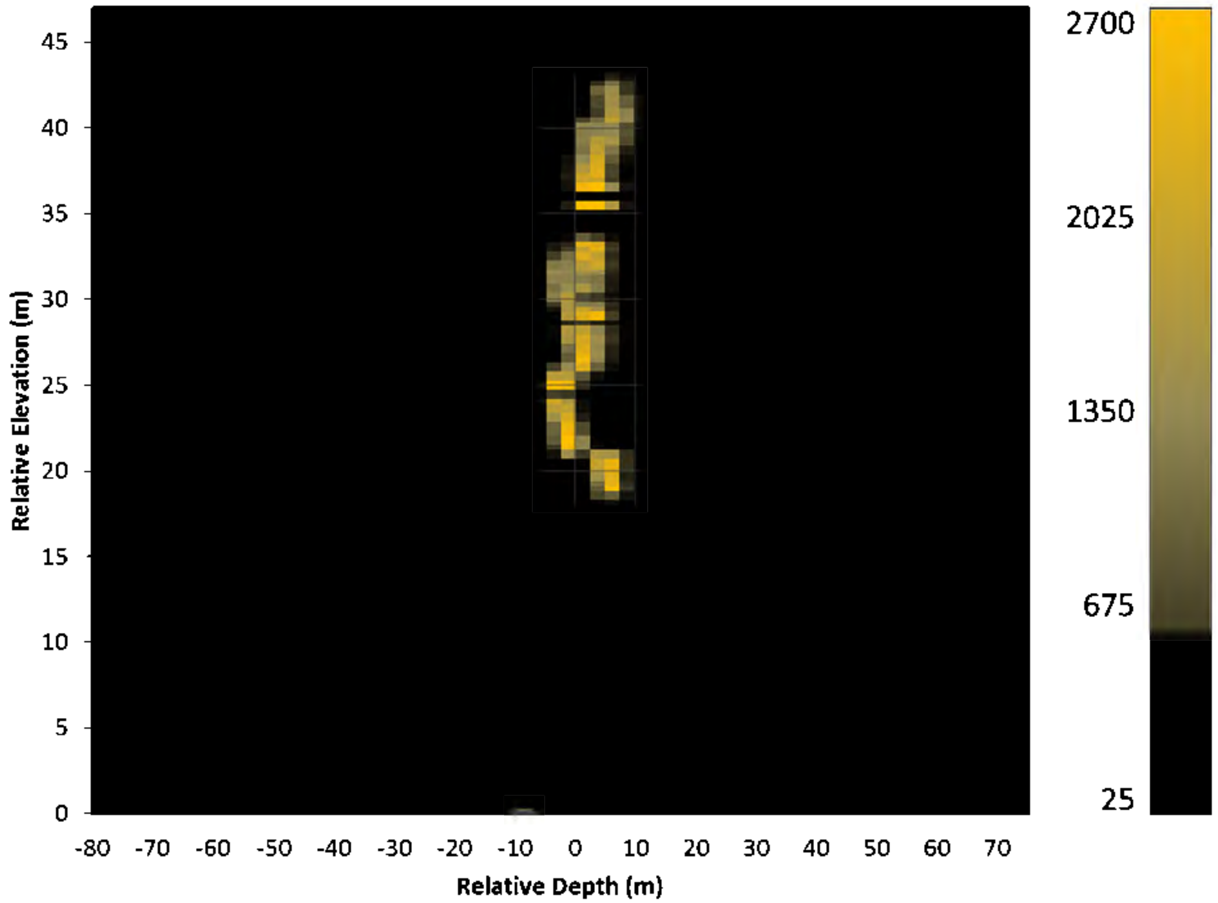

Figure 3-22. Scan above the release point during JRII-8 test, showing the aerosol relative concentration. The color scale indicates the aerosol backscatter photo counts collected in each voxel. The vertical axis is height above the release point, while the horizontal axis is radial distance relative to the release point. This is the RHI collected while the release occurred. The scan started from relative elevation 0 m at 3.74 s prior to the release and ended at a relative elevation of 47 m, 6.3 s after the release. The plume extends continuously between elevation 18 m and 44 m, the four horizontal regions being missed data due to EMI interferences from surrounding equipment.

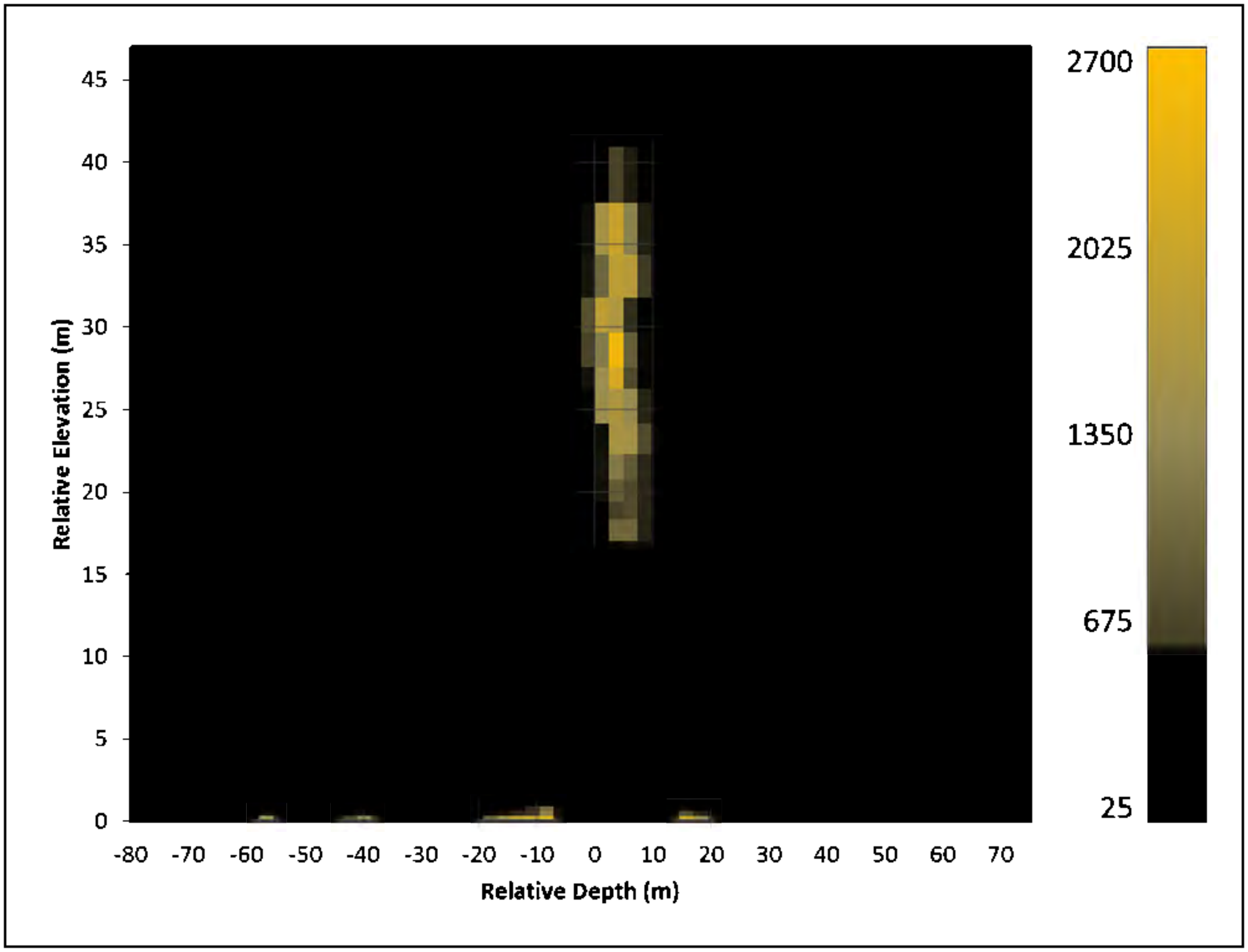

Figure 3-23. Scan above the release point during JRII-8 test, showing the aerosol relative concentration. The color scale indicates the aerosol backscatter photo counts collected in each voxel. The vertical axis is height above the release point, while the horizontal axis is radial distance relative to the release point. This is a RHI retrieved from the fly back and collected after the release occurred. The scan started from relative elevation of 47 m at 6.86 s after the release and ended at a relative elevation of 0 m, 13 s after the release.

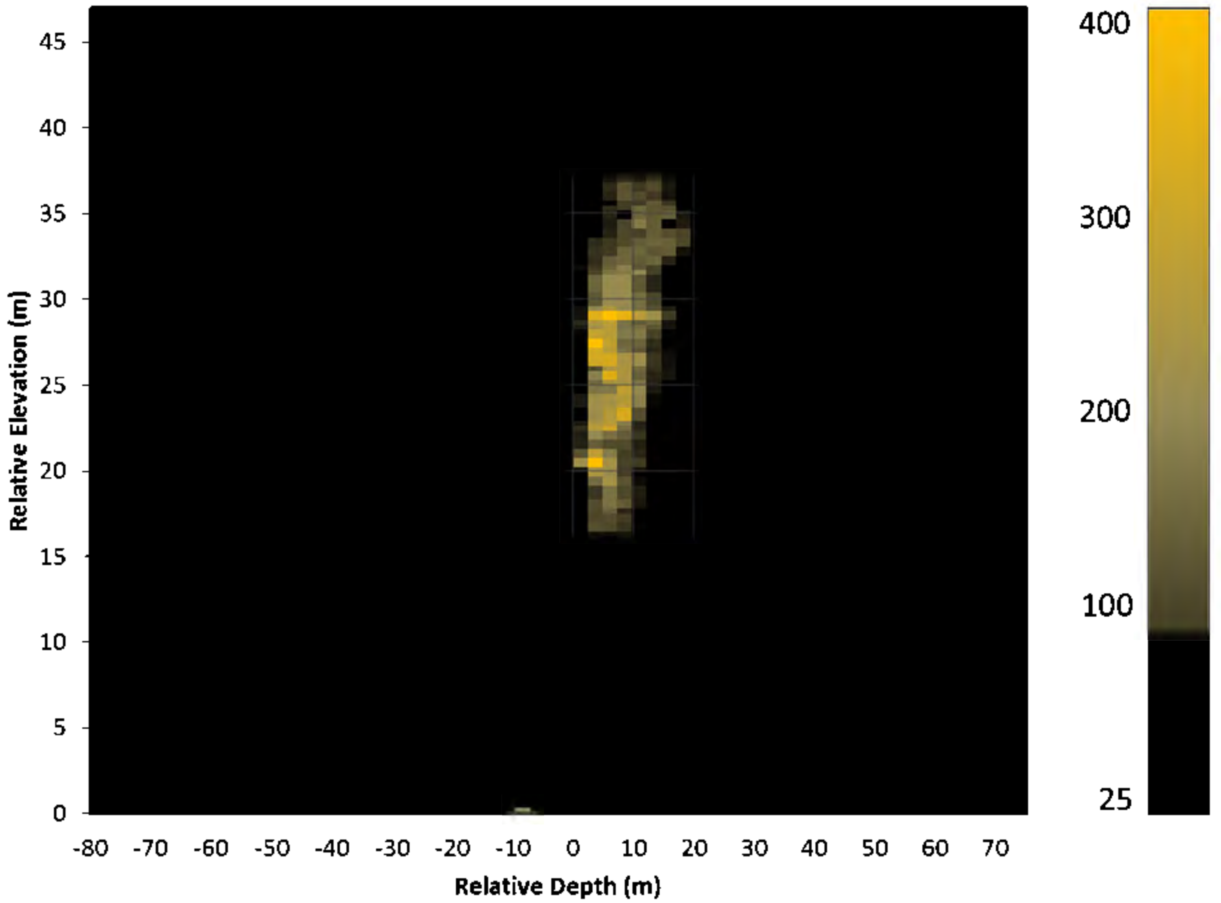

Figure 3-24. Scan above the release point during JRII-8 test, showing the aerosol relative concentration. The color scale indicates the aerosol backscatter photo counts collected in each voxel. The vertical axis is height above the release point, while the horizontal axis is radial distance relative to the release point. This is the second forward RHI collected after the release occurred. The scan started from relative elevation of 0 m at 14 s after the release and ended at a relative elevation of 47 m, 24 s after the release. A different color scaling is used to better visualize the plume.

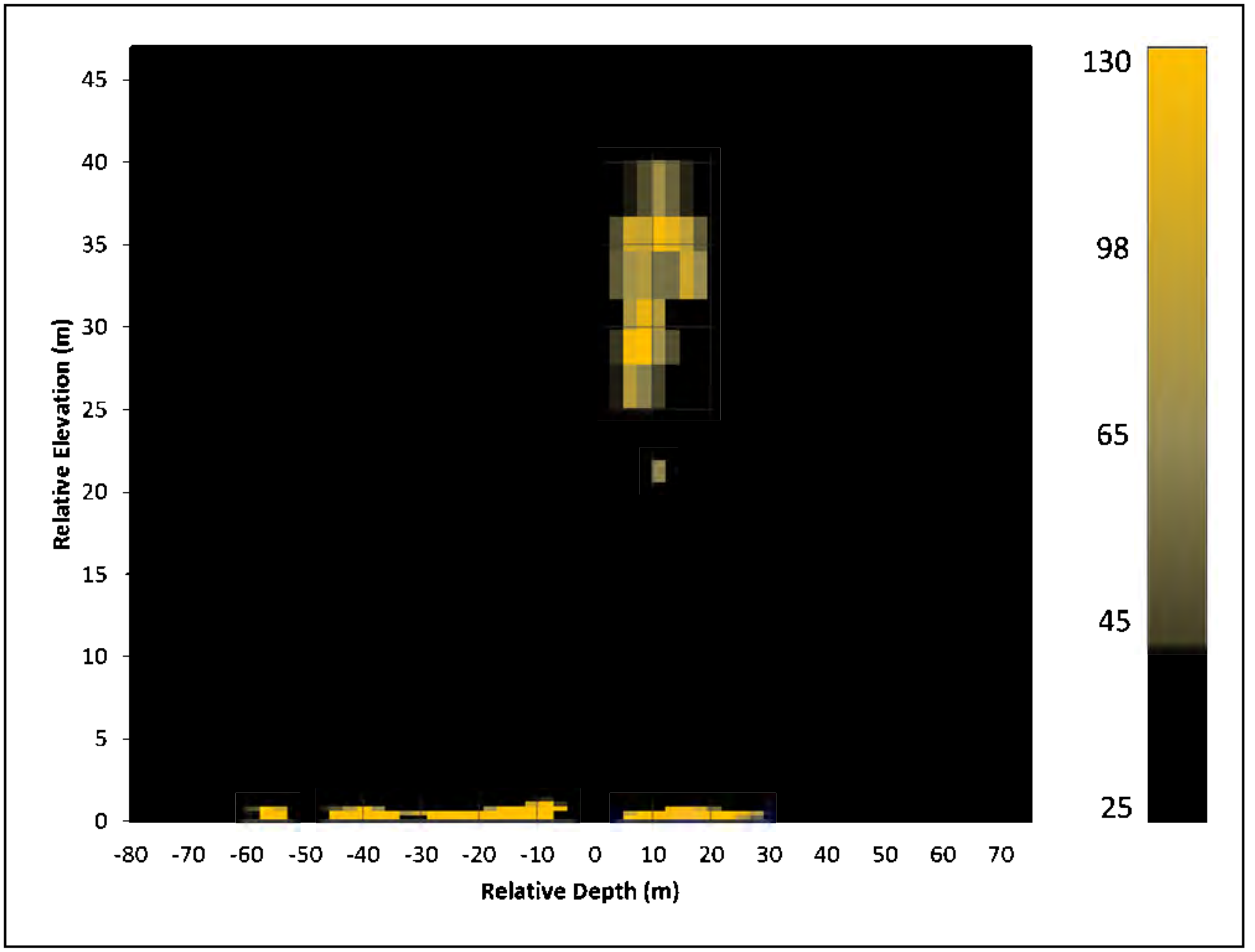

Figure 3-25. Scan above the release point during JRII-8 test, showing the aerosol relative concentration. The color scale indicates the aerosol backscatter photo counts collected in each voxel. The vertical axis is height above the release point, while the horizontal axis is radial distance relative to the release point. This is the second RHI retrieved from a fly back and collected after the release occurred. The scan started from relative elevation of 47 m at 25 s after the release and ended at a relative elevation of 0 m, 31 s after the release. A faint aerosol plume at 27 m above the release point is detectable on this particular scan. A different color scaling is used to better visualize the plume.

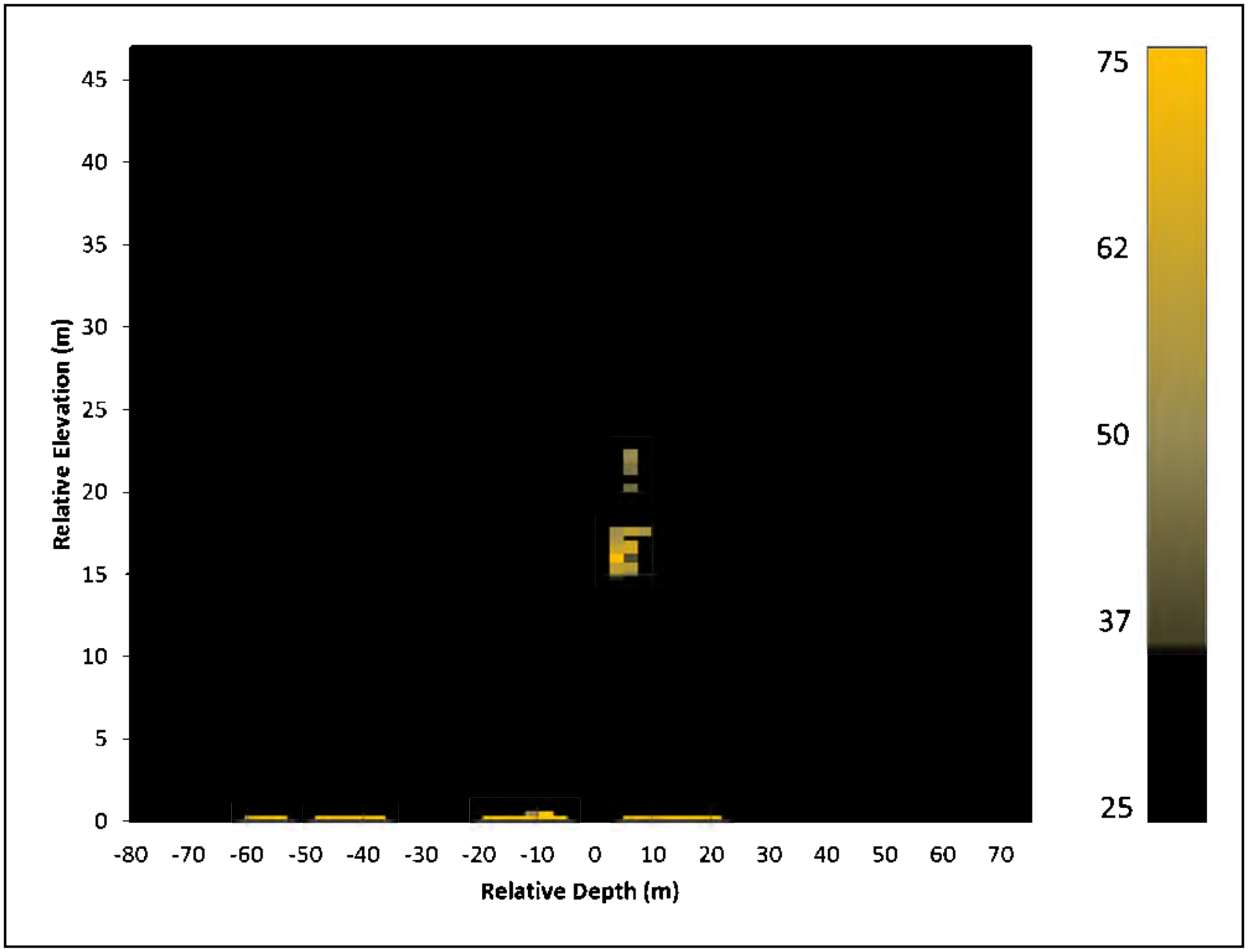

Figure 3-26. Scan above the release point during JRII-8 test, showing the aerosol relative concentration. The color scale indicates the aerosol backscatter photo counts collected in each voxel. The vertical axis is height above the release point, while the horizontal axis is radial distance relative to the release point. This is the fourth forward RHI collected after the release occurred. The scan started from relative elevation of 0 m at 50 s after the release and ended at a relative elevation of 47 m, 60 s after the start of the release. A faint aerosol plume at 16 m above the release point is detectable on this particular scan. A different color scaling is used to better visualize the plume. The previous scan between 32 s and 42 s after the release did not intercept any plume features and is not shown.

From this series of RHIs, we observe that the captured aerosol plume concentration and vertical extent are the largest for the first RHI. In following RHI, the aerosol plume maximum height has decreased and the relative concentration is reduced. This suggests that a strong vertical aerosol plume was created just after the release, and the subsequent RHIs capture the rapid decay of that same aerosol plume. The rapid decay of the aerosol plume height and concentration in the plane just above the release point is probably a combination of aerosol attrition due to gravity fall out and wind advecting the plume outside the vertical scan plane.

We compared the aerosol plume vertical extent collected with REVEAL-5000 with the visible vapor plume collected with a high-resolution video camera. The vertical axis of the video images was calibrated using ImageJ (scientific image analysis) and a scaling reference: the height of the top platform on the camera scaffold (21 ft). In the case of the video image taken at 15:01:50.7 (video time), the maximum height of the visual cloud above the tank in the lidar scan plane is estimated to be 25 m. Figure 3-27 shows the visual cloud extent collected by the camera. The aerosol plume measured by the REVEAL extends well above the visual cloud as shown on the right side of Figure 3-27, indicating that the invisible aerosol plume might follow a different dynamic than the visible vapor cloud.

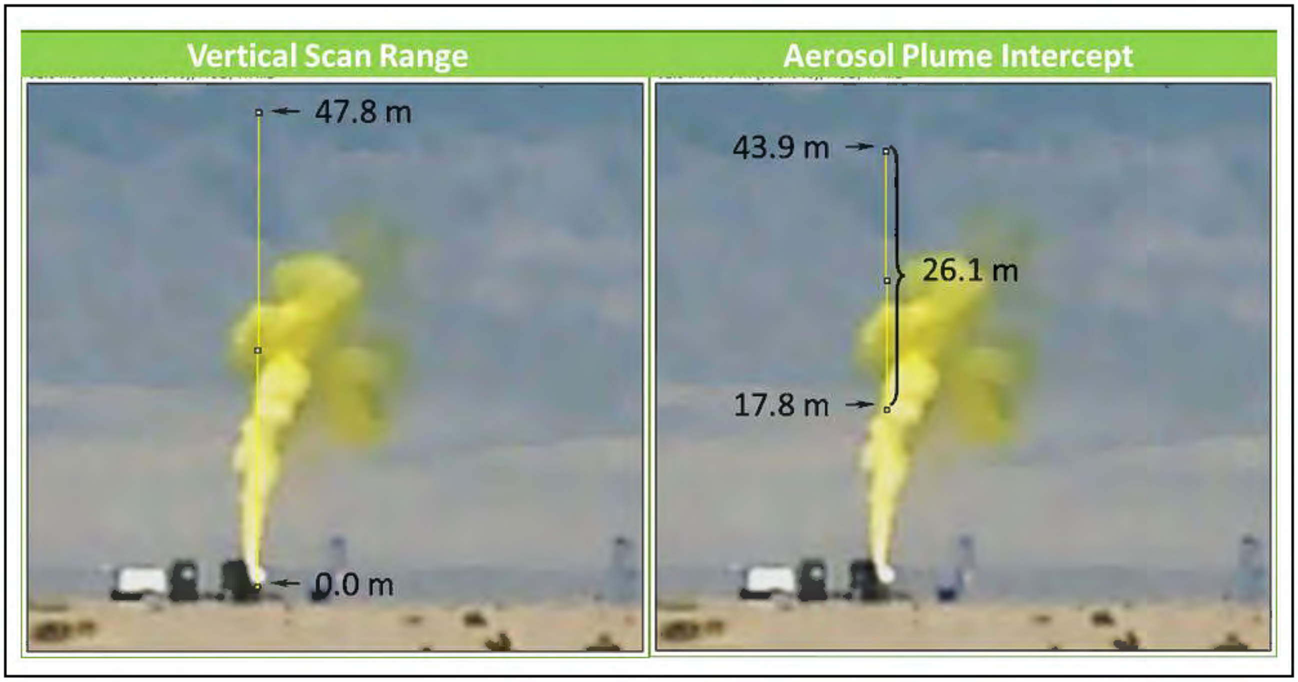

Figure 3-27. Plume images taken with the high-resolution video camera. The vertical span (47.8 m above the tank) of the lidar RHI scan is shown on the left. The vertical extent (26.1 m) of the aerosol plume measured during the first REVEAL-5000 scan is shown on the right.

3.4 JRII-9 Test

Table 3-4. JRII-9 REVEAL configuration quick look summary

Parameter	Value	
Date	17 Sep 2016	
Release start (local time)	08:05:30	
Release stop (local time)	08:10:21	
Released Cl_2 weight (lb)	39,000	
Release orientation from vertical (°)	180	
Wind direction (°)	164.6	
Wind speed (m/s)	3.55	
REVEAL-Prototype status	On site / collecting data	
REVEAL-Prototype scan pattern	PPI scan type 1 at 0.16° elevation	
	Start time	07:30:00
	Stop time	08:07:52
	Start angle	267.28°
	Stop angle	270.21°
	Angular speed	0.123°/s
	PPI scan type 2 at 0.15° elevation	
	Start time	08:08:29
	Stop time	08:34:42
	Start angle	267.28°
	Stop angle	290.27°
	Angular speed	1.92°/s

3.4.1 PPI Type 1 Scans

For the first 2.90 min of this test, REVEAL-Prototype collected type 1 PPIs every 25.80 s (Figure 3-28).

Figure 3-28 is composed of six vignettes representing PPI scans collected over the release pad, each spanning 2.93°. This represents a south–north measured sweep length of 156 m at a range of 3050 m from the REVEAL sensor. Each vignette is a zoomed portion of the collected scan, covering an area of 3000 m × 180 m north of the release point.

The start of the PPI collection time (UTC) is provided above each vignette. The sweep starts from the southernmost point and proceeds clockwise towards the northernmost point. This forward sweep is accomplished in 23.9 s.

The elevation of 0.16° represented a height above the ground around 3 m estimated from the touch down location of the laser beam. This is higher than the height of a standard freight container. In these vignettes the hard-target footprint of two of the video towers are visible. These are represented by the bottom two large white squares in each vignette.

The release of Cl_2 occurred at 14:05:00 UTC with an explosive discharge.

The middle right and bottom two vignettes from Figure 3-28 show a plume that can be attributed to the Cl_2 release. This plume enters the lidar scan sweep at the northeast corner of the southwest tower and propagates towards the north in all the subsequent vignettes.

Figure 3-29 provides a close up and proper rescaling of the relative concentration colors of this middle right graph for clarity. The collection time occurred between 14:06:00 and 14:06:24 UTC. The locations of the release point and the aerosol station are each one indicated by a green pixel with a white frame. The aerosol plume is just south of the aerosol station and is close to intercepting it. In the frame collected between 14:06:26 and 14:06:30 UTC, the plume intercepts the aerosol station.

It is not known if this plume emerged from the bottom to intercept the lidar scanning plane or if it came from the top. Further analysis correlating this frame with the high-resolution video should provide further insight.

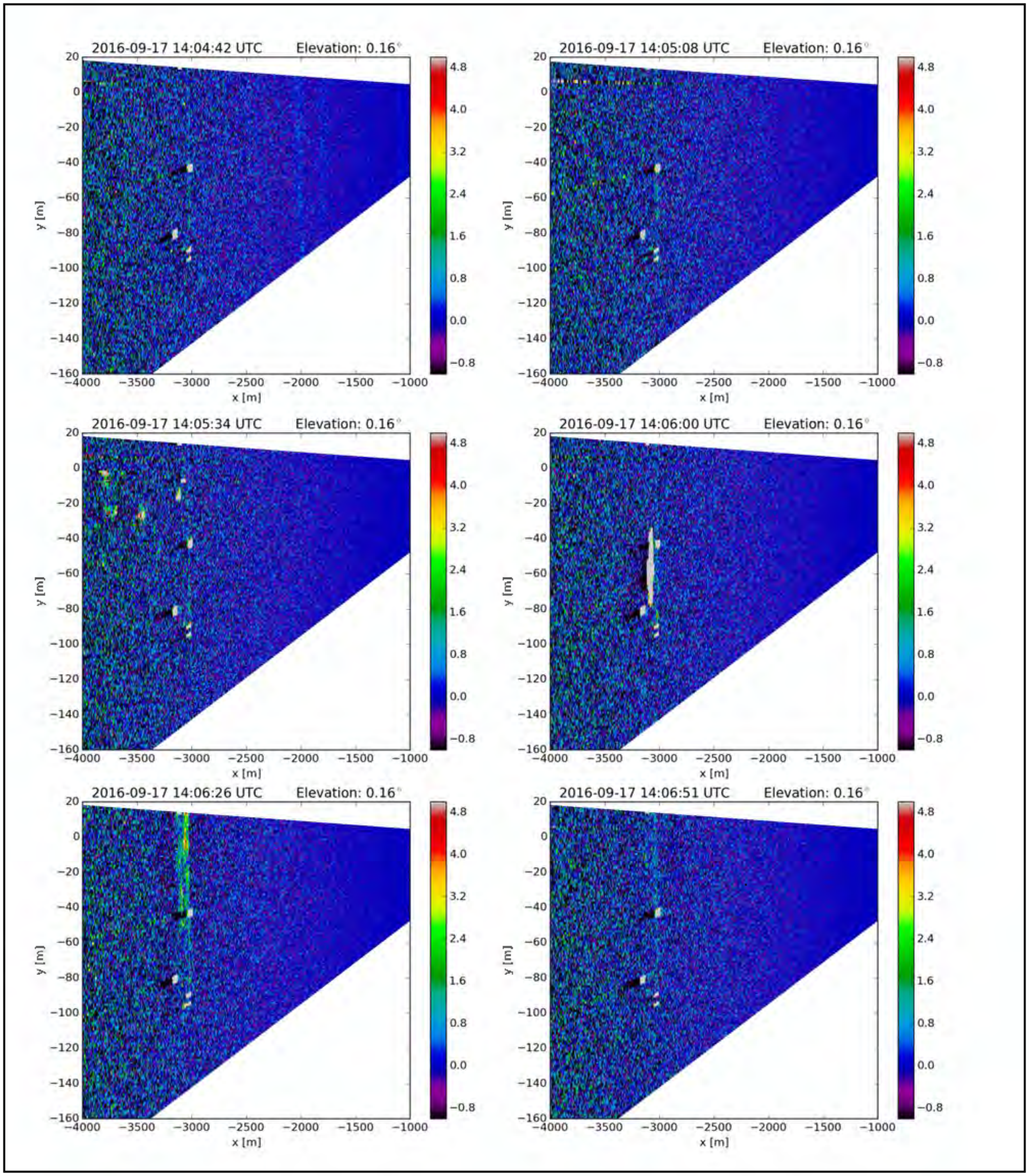

Figure 3-28. PPI scans above the release pad during the JRII-9 test. UTC time on top of each graph is start time of the scan; stop time of the scan is 23.9 s later.

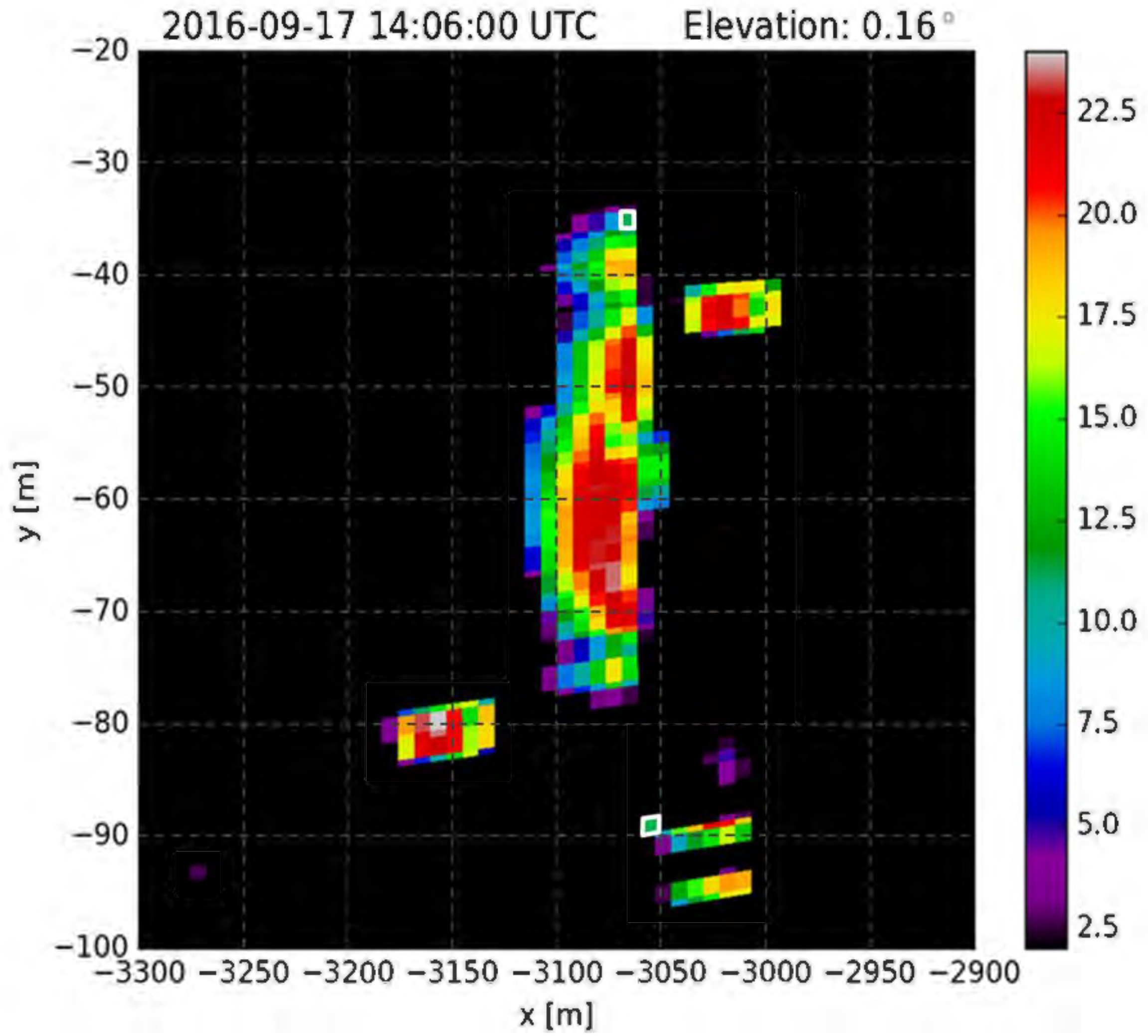

Figure 3-29. Same PPI scan above the release pad during the JRII-9 test data as the one shown in the middle right vignette of Figure 3-28, plotted on a different color scale for clarity. The locations of the release point and the aerosol station are each one indicated by a green pixel with a white frame. The aerosol plume is just south of the aerosol station and is close to intercepting it (see Appendix A: Aerosol Arrival and Departure Time Analysis Using REVEAL Data for revised arrival time).

3.4.2 PPI Type 2 Scans

After the PPI type 1 scans and for the following 26 min of this test, REVEAL-Prototype collected type 2 PPIs every 25.3 s (Figure 3-30 and Figure 3-31).

Figure 3-30 and Figure 3-31 are each composed of six vignettes representing PPI scans collected over the release pad and north of the release pad, each spanning 22.99°. This represents a south–north measured sweep length of 1294 m at a range of 3050 m from the REVEAL sensor. Each vignette is a zoomed portion of the collected scan, covering an area of 3000 m × 1660 m north of the release point.

The start of the PPI collection time (UTC) is provided above each vignette. The sweep starts from the southernmost point and proceeds clockwise towards the northernmost point. This forward sweep is accomplished in 23.8 s.

In each of the graphs, we can see a delta-shaped aerosol plume resulting from the explosive release that propagates from the release pad towards the north.

In section 3.4.3 (Analysis 3 – Propagation Speed of the Aerosol Plume), we will use this plume to infer the ground speed and heading of this aerosol cloud.

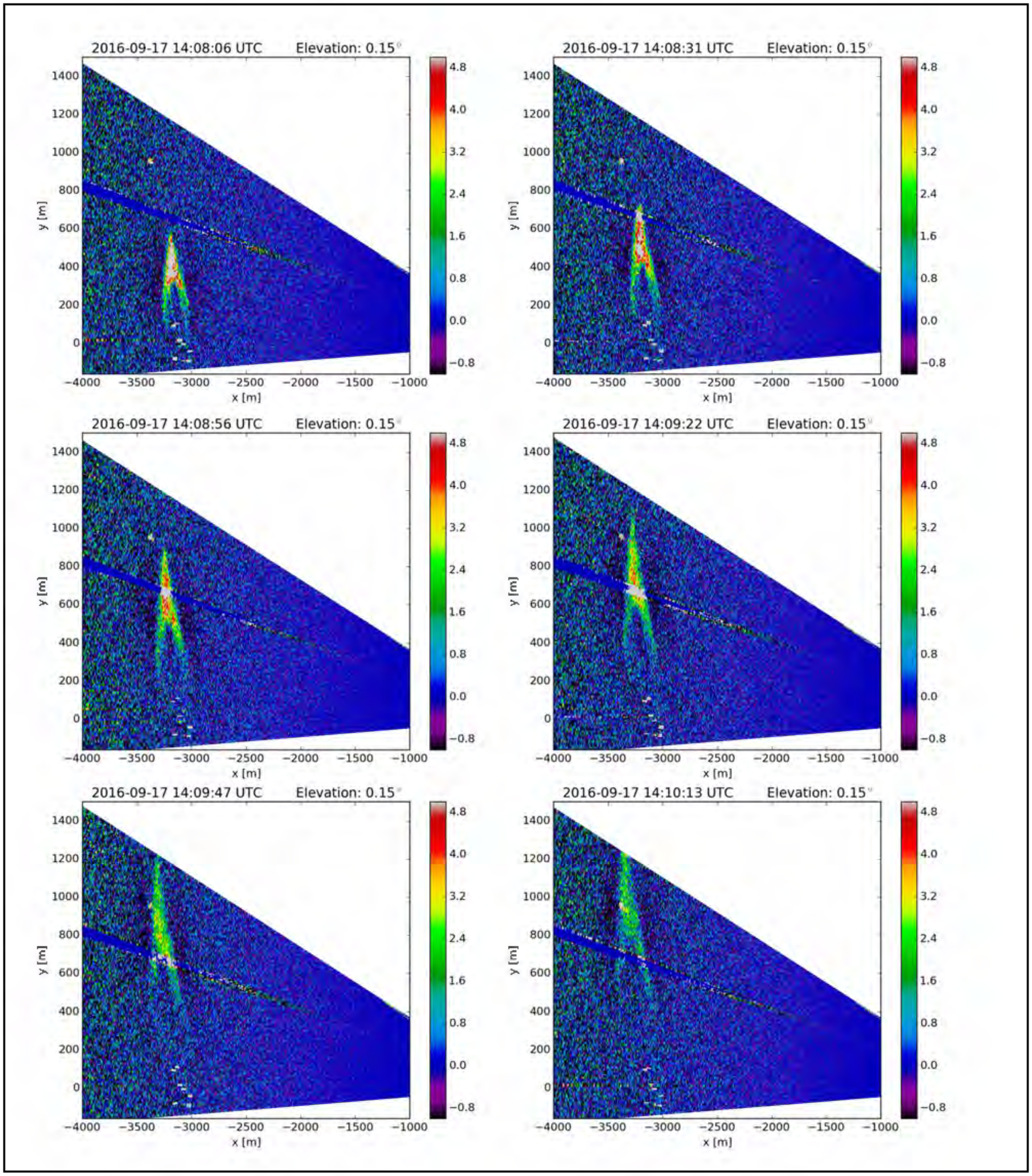

Figure 3-30. PPI scans north of the release pad during the JRII-9 test. UTC time on top of each graph is start time of the scan; stop time of the scan is 24 s later.

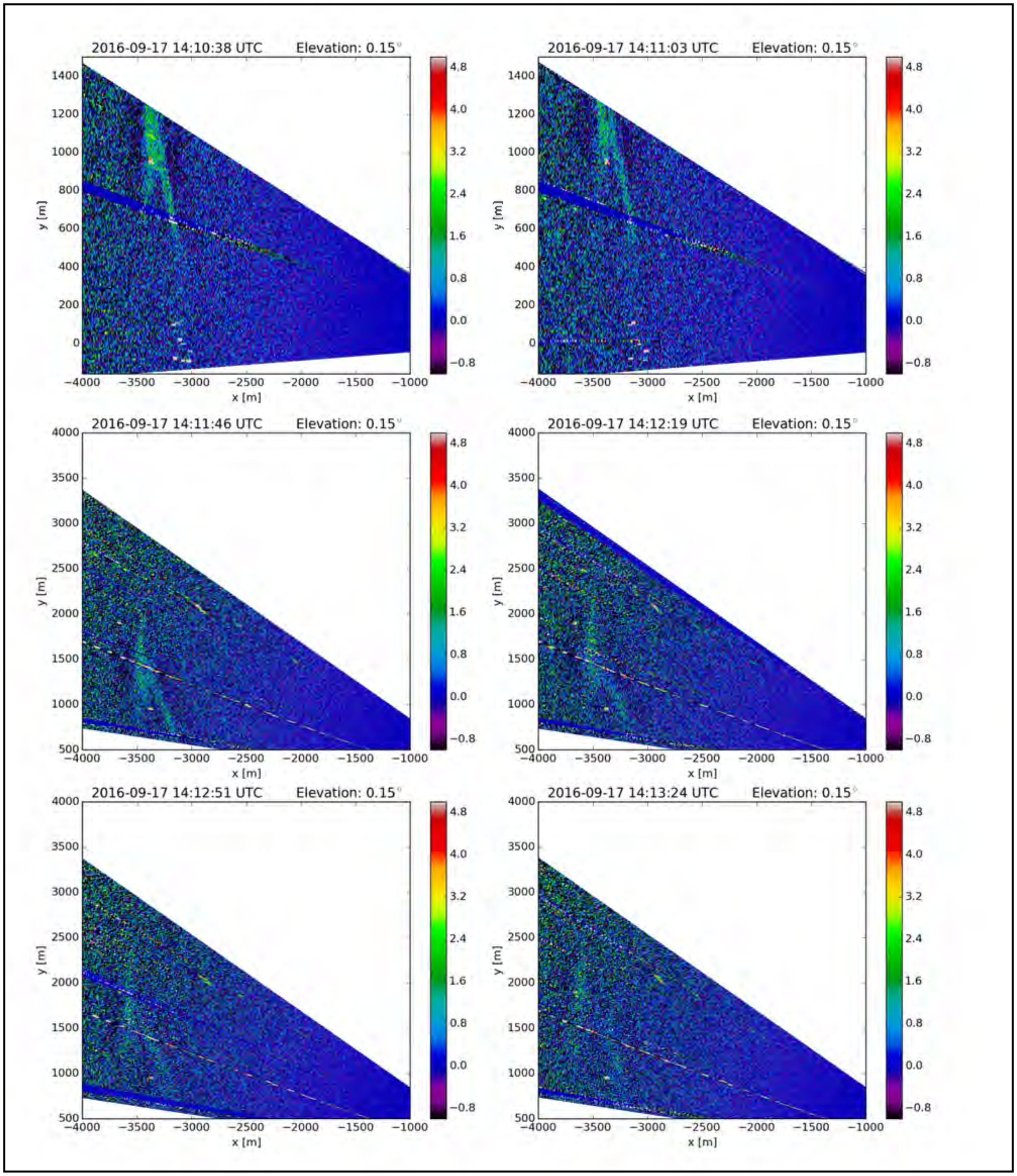

Figure 3-31. PPI scans north of the release pad during the JRII-9 test. UTC time on top of each graph is start time of the scan; stop time of the scan is 24 s later.

3.4.3 Analysis 3 – Propagation Speed of the Aerosol Plume

We used two methods to retrieve the ground velocity of the aerosol cloud emerging from the release pad.

The first one uses a pattern-matching technique to infer the distance travelled by the aerosol cloud between two successive frames. In order to minimize the overall residual differences between two successive frames, each frame was rescaled and translated. The amount of required translation to reach this minimum provided an estimation of the distance travelled. This was implemented postcollection on a frame-to-frame basis to provide a supervised and high confidence analysis.

The second method uses the recorded results from the embedded optical flow algorithm that analyses the lidar frames real time as they were being generated, to infer the wind field best matching the data in a fully automated process.

The two methods were compared in order to verify that both provide the same quantitative assessment of the cloud velocity.

Figure 3-32 shows the five PPI scans selected to conduct the analysis and Figure 3-33 shows the five plumes overlaid with the measured plume horizontal translation between each frame quantified.

Table 3-5 summarizes the results from the cross-correlation technique. The average plume ground speed measured using this technique is 4.5 m/s, while the cloud direction is 163°. Note that the plume ground speed retrieved with this technique is at the height probed by the REVEAL line of sight, corresponding to a height above ground of approximately 4 m. The tower met sensor mean wind velocity at a 4 m height 8 min after the release is close to a value of 4 m/s, which is in relatively good agreement.

Figure 3-34 shows a summary of the wind fields inferred by the optical flow algorithm technique during the tests. Table 3-6 provides a summary of the corresponding results. The variability of the results obtained with the optical flow technique is greater. The average ground speed is found to vary between 4.2 and 4.65 m/s while the cloud direction varies between 166° to 161°. Nonetheless these two set of measurements are remarkably close, both suggesting that the aerosol cloud ground velocity is close to 4.5 m/s.

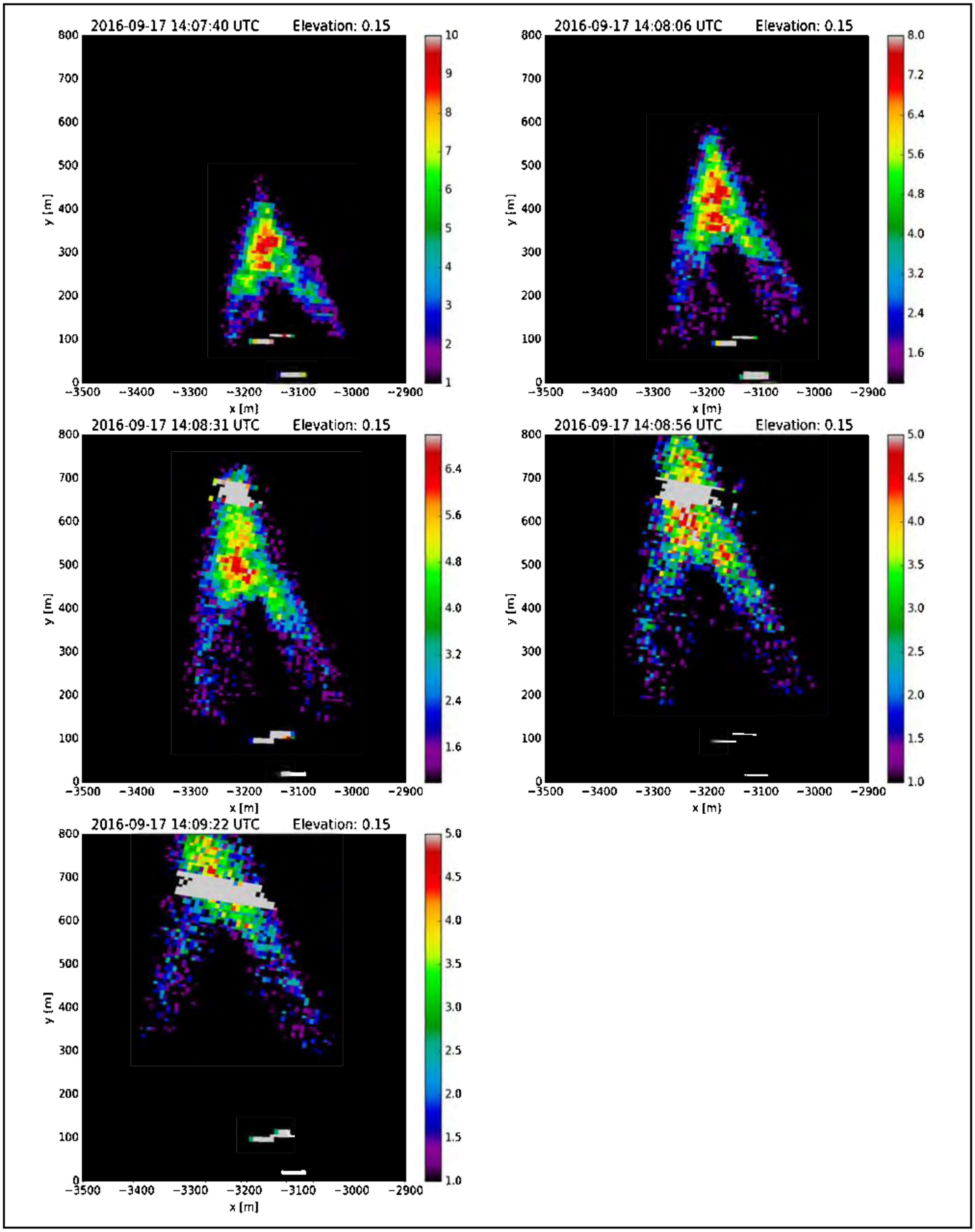

Figure 3-32. PPI scans during JRII-9 test, used to derive the plume velocity. The displacement of the delta-shaped plume between each frame is used to infer the overall plume ground velocity.

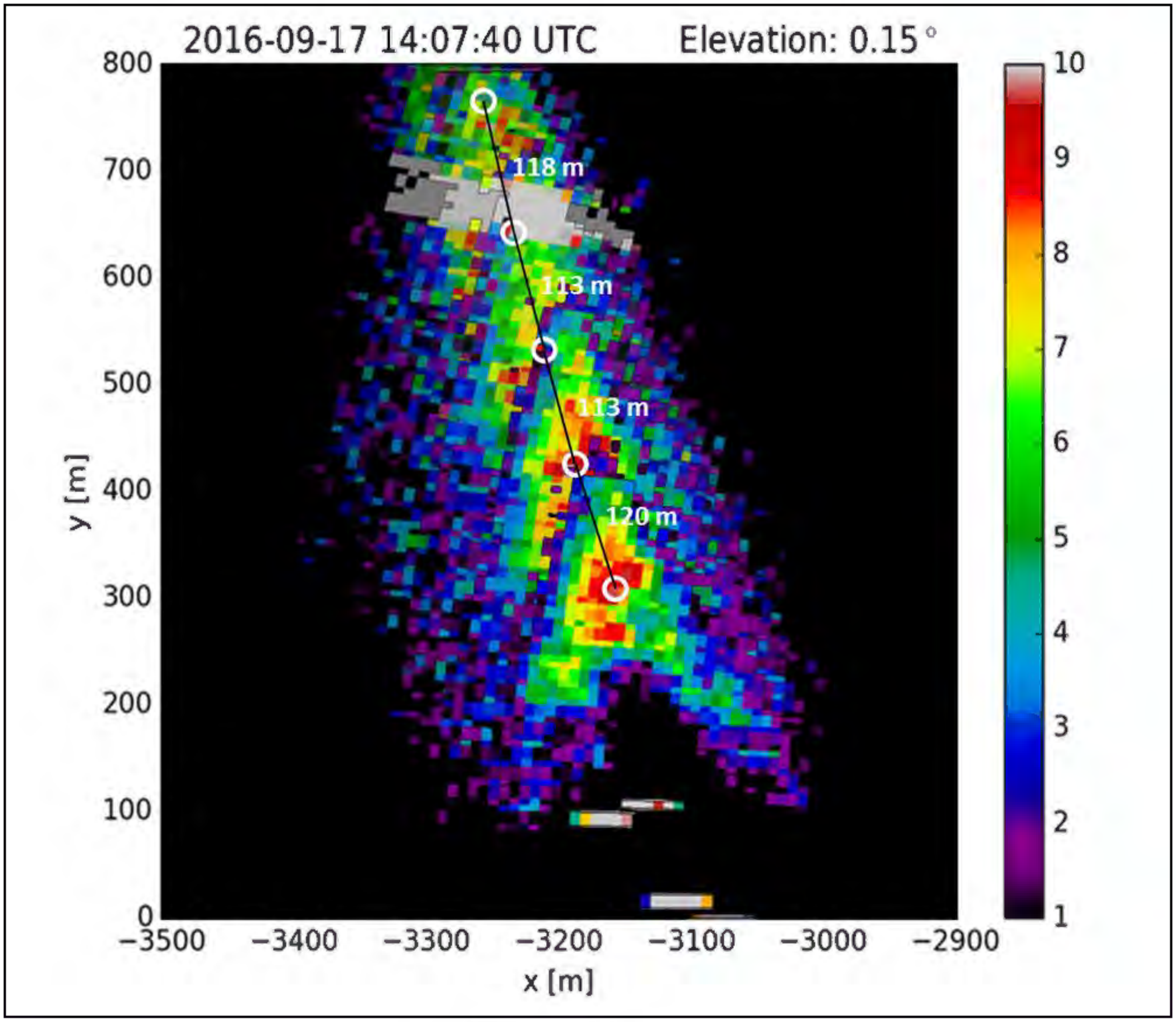

Figure 3-33. The five frames presented in Figure 3-32 (JRII-9) are overlaid and the measured translation using a pattern-matching technique between successive frames is shown

Table 3-5. Results from the pattern-matching technique. For each couple of successive frames, the table provides the time between each frame, the distance travelled, the ground speed, and the cloud direction.

Segment	Δt (s)	ΔL (m)	Speed (m/s)	Theta (°)
1 to 2	26	119.67	4.60	160.46
2 to 3	25	113.11	4.52	163.69
3 to 4	25	112.57	4.50	164.09
4 to 5	26	118.16	4.54	165.44

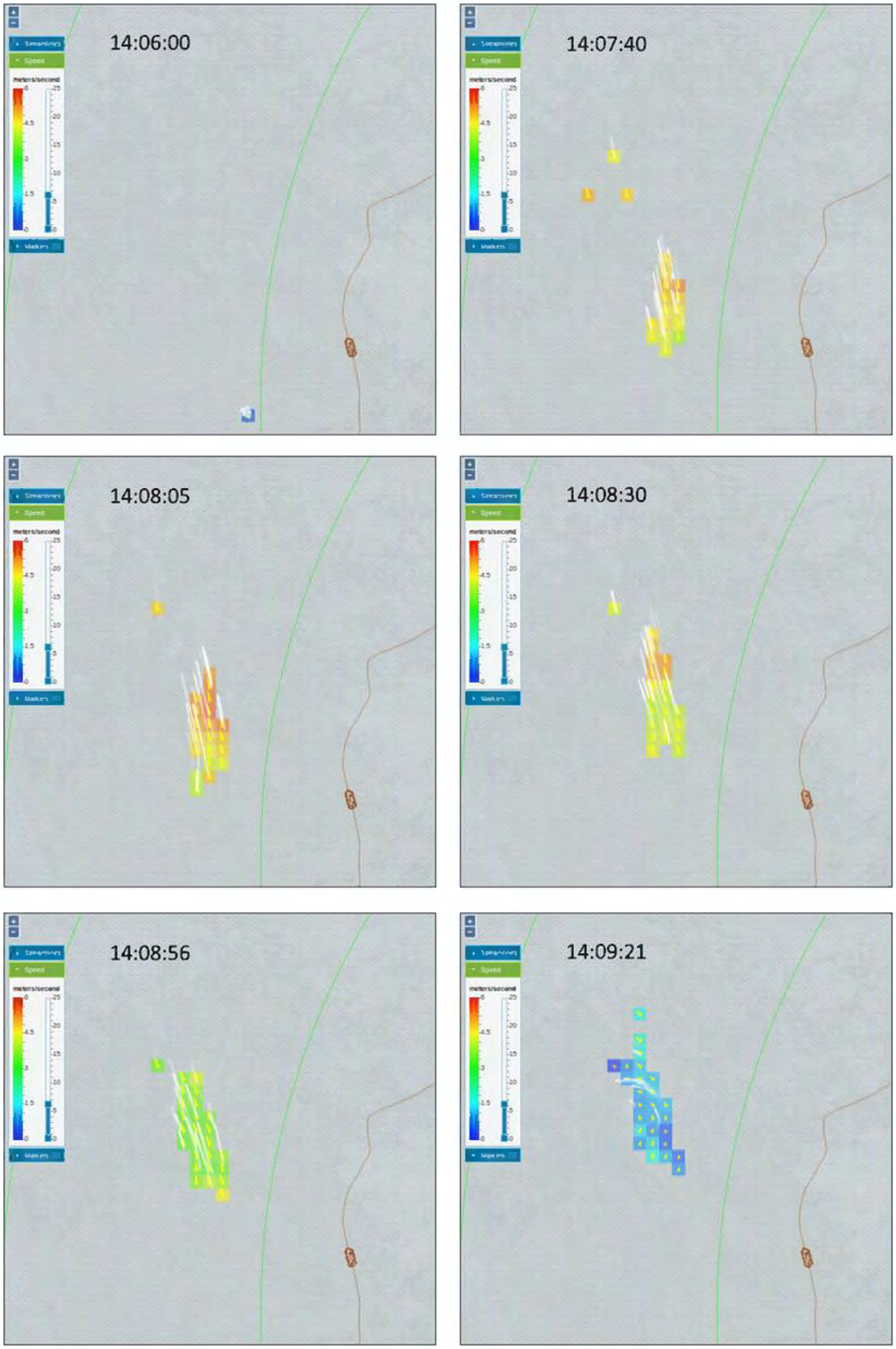

Figure 3-34. Corresponding wind fields (JRII-9) calculated by the real-time optical flow algorithm

Table 3-6. Results from optical flow technique. For each couple of successive frames, the ground speed and the wind direction is given.

Segment	Speed (m/s)	Direction (°)
1 to 2	4.1 to 4.9, avg 4.5	166
2 to 3	4.1 to 5.1, avg 4.65	166
3 to 4	4.0 to 4.9, avg 4.45	164
4 to 5	3.9 to 4.5, avg 4.2	161

4.0 Summary and Conclusions

This report presented the data collected by both the REVEAL-Prototype system and the REVEAL-5000 system during the 2016 JRII set of 4 tests. In each test, REVEAL data was able to provide additional insight into the morphology and dynamics of the associated aerosol plumes.

During the JRII-6 test, the REVEAL-Prototype did not perform optimally due to a poor configuration of the sensor scanning parameters. Scanning speed was too high providing lower sensitivity and low angular resolution. Elevation angle was too high and provided few episodes of cloud intercepts with the sensor FOR.

During the JRII-7 test, the REVEAL-Prototype performed better due to a readjustment of the scanning speed. This provided improved angular resolution compared to the first test. Lowering the scan elevation improved the cloud intercept conditions, and an opportunity to map the relative concentration on the release pad did occur.

During the JRII-8 test, both the REVEAL-Prototype and the REVEAL-5000 operated in concert. The REVEAL-Prototype operated on the same PPI scans as in previous tests but with an even smaller elevation height, providing an intercept plane very close to the release pad height. This provided the conditions to collect the aerosol plume touch down location. The REVEAL-5000 operated in parallel and scanned vertically (RHI) directly above the release point, documenting the vertical relative concentration of ejected aerosols in that plane.

During the JRII-9 test, the REVEAL-Prototype operated on the same initial PPI but at slightly higher scanning elevation. This provided an opportunity to map the relative aerosol concentration on the release pad. The REVEAL-Prototype then switched to broader PPI scans and was able to map the aerosol cloud exiting the release pad. By conducting an analysis on this cloud, it was concluded that this aerosol plume was traveling at speeds close to 4.5 m/s.

Some problems and opportunities for improvement were also noted. The aerosol lidar contribution to the documentation of the aerosol plume associated with the Cl_2 release suffered from interfering ambient aerosol plumes generated from the dust covering the access roads. Dust control measures such as water spraying before the release could have mitigated this issue. On several occasions, lidar data were lost due to interfering electronic noise generated by radios or surrounding equipment. Precisely controlling the laser beam height above the release pad proved tricky. As ambient temperature quickly rises during early morning hours, the laser beam undergoes refractive bending causing this height to change. A procedure to correct for these refractive-index gradient changes would allow stabilizing and therefore properly calibrating the sensor FOR height above the ground.

Appendix A Aerosol Arrival and Departure Time Analysis Using REVEAL Data

A.1 Background

S3 deployed two eye-safe elastic aerosol-backscatter lidar systems called Real-time Eye-safe Visualization, Evaluation, and Analysis Lidar (REVEAL) to provide additional data supporting the characterization of the releases. The first system, REVEAL-Prototype is the first generation system and was deployed in previous field tests at DPG. The second system, REVEAL-5000 is a more highly engineered version of the REVEAL and was developed and integrated just prior to these tests. The REVEAL-Prototype was in operation and collected data during the four releases that occurred on 31 August 2016 (JRII-6), 3 September 2016 (JRII-7), 11 September 2016 (JRII-8), and 17 September 2016 (JRII-9). The REVEAL-5000 was deployed later and collected data during JRII-8.

The REVEAL systems were located just to the north of the CP at a latitude of 40.135162° and a longitude of –113.451375°. This placed the systems at a range of 3065 m from the aerosol station with a bearing of 269.32°. The systems performed most of their scans in the vicinity of the aerosol station to try to collect aerosol data that could be correlated with data from the point sensors at the station. A detailed description of the REVEAL deployment configuration and measurement results is contained in the main body of this report.

A.2 Analysis Results

To create a dimensionally correct representation of the data, the REVEAL sector scan data associated with horizontal scans are displayed as PPIs where the range and bearing (azimuth angle) information are used to position each voxel as color-coded pixels in a radial or Cartesian 2-D plot. We refer to figures in the report containing these PPI "images" of the aerosols from each of the trials to determine the arrival and departure time of the aerosols to and from the station, respectively. The time at the top of each PPI plot is the start time for that PPI scan. The REVEAL beam intercepts the aerosol station at the end of the scan in Trial 6. In Trial 7 and 8, the REVEAL beam intercepts the aerosol station at 50.5% of the way into each scan. Finally, in Trial 9 the azimuth scans were started at a value 1° below previous scans, and the REVEAL beam intercepts the aerosol station at 68.3% of the way into each scan. Thus, we calculate the arrival time by taking the PPI start time and adding these scans lag times.

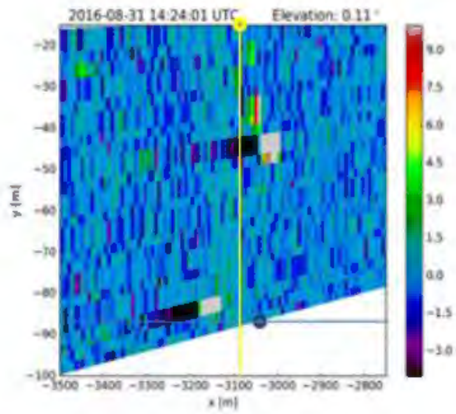

Trail 6

The aerosols are 5 m south of the station (85-3) in the lower left-hand PPI plot in Figure 3-1.

Release time (RT) = 14:23:35

Scan duration = 3 s

Additional time to reach station = 5 m / 2.5 m.s^{-1}

Arrival time = 14:24:01 + 3 s + 2 s = 14:24:06 (31 s after RT)

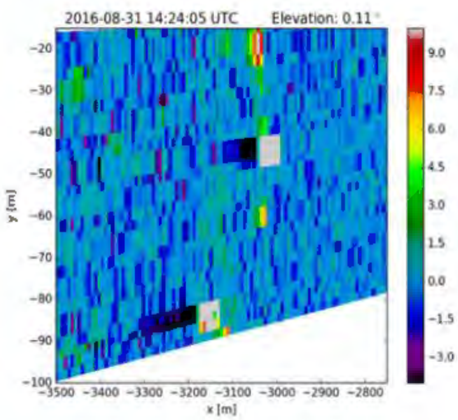

The aerosols depart from the station between Time 1 corresponding to the lower right-hand PPI plot in Figure 3-1 and Time 2 corresponding to the PPI graph collected 5 s after this graph.

Time 1 = 14:24:05 + 3 s = 14:24:08

Time 2 = 14:24:10 + 3 s = 14:24:13

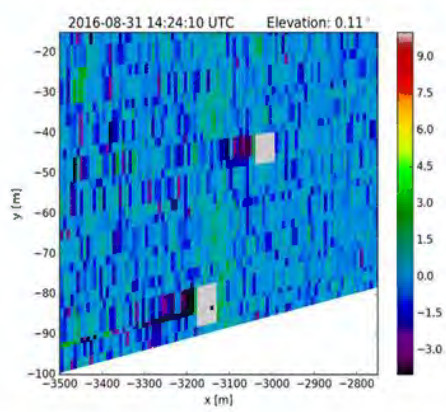

If we assume an average wind of 2.5 m.s^{-1} and that the aerosol plume has to travel and additional 10 m to clear the station, the projected departure time is:

Departure time = 14:24:08 + 10/2.5 s = 14:24:12 (37 s after RT)

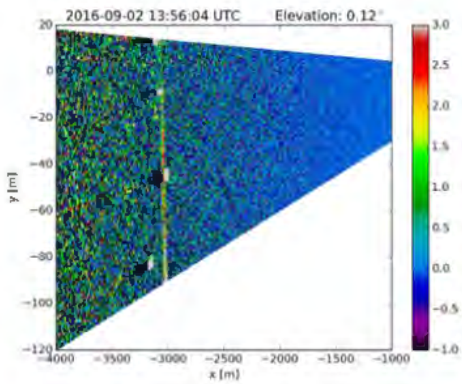

Trial 7

The aerosols arrive at the station (southeast corner) in the upper right-hand PPI plot in Figure 3-5.

RT = 13:56:00

Each scan duration is 21 s and the time required to reach the aerosol station after start of scan is 11 s.

Arrival time = 13:56:04 + 11 s = 13:56:15 (15 s after RT)

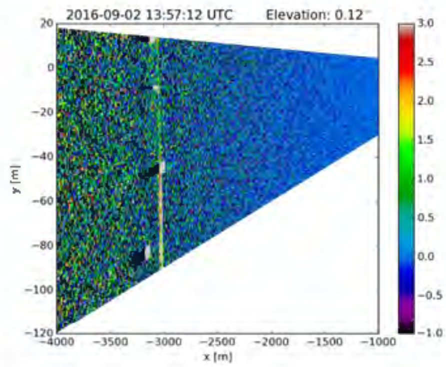

The aerosols depart from the station in the lower left-hand PPI plot in Figure 3-5.

Departure time = 13:57:12 + 11 s = 13:57:23 (83 s after RT)

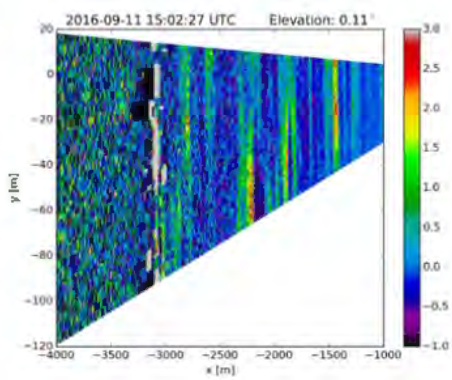

Trial 8

The aerosols arrive at the station in the lower right-hand PPI plot in Figure 3-7 (also see the RTI plot in Figure 3-16).

RT = 15:01:45

Each scan duration is 9 s and the time required to reach the aerosol station after start of scan is 4.5 s.

Arrival Time = 15:02:27 + 4 s = 15:02:31 (46 s after RT)

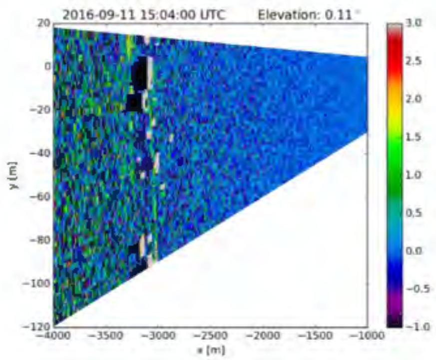

The aerosols depart from the station in the middle left-hand PPI plot in Figure 3-9.

Departure time = 15:04:00 + 4 s = 15:04:04 (139 s after RT)

This departure was difficult to judge because the aerosols after 15:03:08 (see middle right-hand plot in Figure 3-8) look like they could be residual dust. In this case the departure time is:

Departure time = 15:03:08 + 4 = 15:03:12 (87 s after RT)

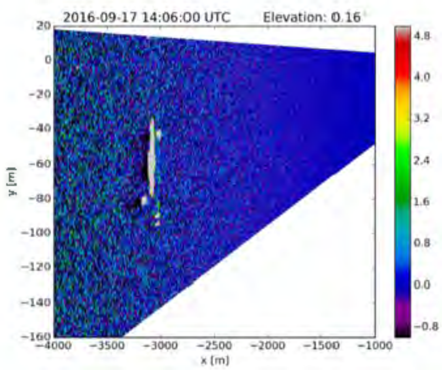

<u>Trial 9</u>

The aerosols arrive at the station in the middle right-hand PPI plot in Figure 3-28 (also see the RTI plot in Figure 3-29).

RT = 14:05:30

Each scan duration is 24 s and the time required to reach the aerosol station after start of scan is 16 s.

Arrival time = 14:06:00 + 16 s = 14:06:16 (46 s after RT)

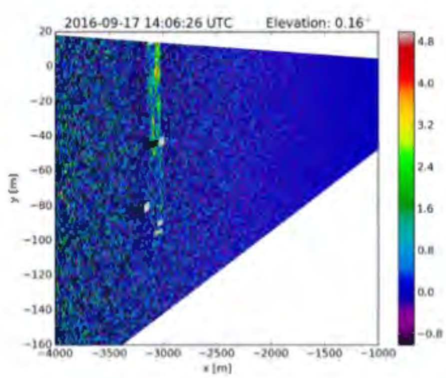

The aerosols depart from the station in the lower left-hand PPI plot in Figure 3-28.

Departure time = 14:06:26 + 16 s = 14:06:42 (72 s after RT)

Acronyms and Conversions

This section includes the list of acronyms and the conversion table.

List of Acronyms

Acronyms	
CP	command post
CSAC	Chemical Security Analysis Center
DHS	Department of Homeland Security
DPG	Dugway Proving Ground
DTRA	Defense Threat Reduction Agency
FOR	field of regard
JRII	Jack Rabbit II
PPI	Plan Position Indicator
PRF	pulse repetition frequency
REVEAL	Real-time Eye-safe Visualization, Evaluation, and Analysis Lidar
RHI	Range Height Indicator
RT	release time
RTI	Range Time Indicator
S3	Spectral Sensor Solutions
S/K	Sophos/Kydoimos
2-D	two dimensional
WMD	weapons of mass destruction

Conversion Table

This table includes conversion factors for changing US customary measures to metric (SI) units of measurement, and vice versa.

Multiply US	———>	by Conversion	———>	To Get SI
To Get US	———>	by Conversion	———>	Divide SI

US Measurement	Conversion	SI Measurement
angstrom	$1.000\,000 \times 10^{-10}$	meters (m)
atmosphere (normal)	$1.013\,250 \times 10^{2}$	kilopascal (kPa)
bar	$1.000\,000 \times 10^{2}$	kilopascal (kPa)
barn	$1.000\,000 \times 10^{-28}$	meter^2 (m^2)
British thermal unit (thermochemical)	$1.054\,350 \times 10^{3}$	joule (J)
calorie (thermochemical)	4.184 000	joule (J)
cal (thermochemical/cm^2)	$4.184\,000 \times 10^{-2}$	megajoule/m^2 (MJ/m^2)
curie	$3.700\,000 \times 10^{1}$	gigabecquerel (GBq)*
degree (angle)	$1.745\,329 \times 10^{-2}$	radian (rad)
degree Fahrenheit	$T_K = (T_F + 459.67)/1.8$	Kelvin (K)
electron volt	$1.602\,177 \times 10^{-19}$	joule (J)
erg	$1.000\,000 \times 10^{-7}$	joule (J)
erg/second	$1.000\,000 \times 10^{-7}$	watt (W)
foot	$3.048\,000 \times 10^{-1}$	meter (m)
foot-pound-force	1.355 818	joule (J)
gallon (US liquid)	$3.785\,412 \times 10^{-3}$	meter^3 (m^3)
inch	$2.540\,000 \times 10^{-2}$	meter (m)
jerk	$1.000\,000 \times 10^{9}$	joule (J)
joule/kilogram (J/kg) radiation dose absorbed	1.000 000	gray (Gy)**
kilotons	4.183	terajoules

US Measurement	Conversion	SI Measurement
kip (1000 1bf)	$4.448\ 222 \times 10^{3}$	newton (N)
kip/inch^2 (ksi)	$6.894\ 757 \times 10^{3}$	kilopascal (kPa)
ktap	$1.000\ 000 \times 10^{2}$	newton-second/m^2 (N·s/m^2)
micron	$1.000\ 000 \times 10^{-6}$	meter (m)
mil	$2.540\ 000 \times 10^{-5}$	meter (m)
mile (international)	$1.609\ 344 \times 10^{3}$	meter (m)
ounce	$2.834\ 952 \times 10^{-2}$	kilogram (kg)
pound-force (lbf avoirdupois)	4.448 222	newton (N)
pound-force inch	$1.129\ 848 \times 10^{-1}$	newton-meter (N·m)
pound-force/inch	$1.751\ 268 \times 10^{2}$	newton/meter (N/m)
pound-force/foot^2	$4.788\ 026 \times 10^{-2}$	kilopascal (kPa)
pound-force/inch^2 (psi)	6.894 757	kilopascal (kPa)
pound-mass (lbm avoirdupois)	$4.535\ 924 \times 10^{-1}$	kilogram (kg)
pound-mass-foot^2 (moment of inertia)	$4.214\ 011 \times 10^{-2}$	kilogram-meter^2 (kg·m^2)
pound-mass/foot^3	$1.601\ 846 \times 10^{1}$	kilogram/meter^3 (kg/m^3)
rad (radiation dose absorbed)	$1.000\ 000 \times 10^{-2}$	gray (Gy)**
rem (roentgen equivalent man)	$1.000\ 000 \times 10^{-2}$	sievert (Sv)***
roentgen	$2.579\ 760 \times 10^{-4}$	coulomb/kilogram (C/kg)
shake	$1.000\ 000 \times 10^{-10}$	second (s)
slug	$1.459\ 390 \times 10^{1}$	kilogram (kg)
torr (mmHg, 0 ºC)	$1.333\ 22 \times 10^{-1}$	kilopascal (kPa)

* The becquerel (Bq) is the SI unit of radioactivity; 1 Bq = 1 event/s.
** The gray (Gy) is the SI unit of absorbed radiation.
*** The sievert (Sv) is the SI unit of dose equivalent.

DTRA/SCC-WMD Scientific & Technical Review Information J9 16-1316

1. PA CONTROL NUMBER: 17-264 3/21/17 — 1a. SUSPENSE: ~~Nov 3, 2016~~ 31 May
2. PM / PHONE / EMAIL: Bruce Hinds 5058535722 — 2a. DATE: Nov 9, 2016
3. BRANCH CHIEF / PHONE /EMAIL: LTC Jeff Moran/ 505- 846-6590 — 3a. DATE:
4. DIVISION CHIEF / PHONE: Dr. Gary Hook/ 505-846-5513 HOOK.GARY.L EE.1084831279 — 4a. DATE: Nov 9, 2016
5. DEPARTMENTS / PHONE: — 5a. DATE:
6. JDir/ OFFICE / PHONE: Tom Niner X 3021 NINER.THOMAS.W.1272926987 Digitally signed by NINER.THOMAS.W.1272926987 DN: c=US, o=U.S. Government, ou=DoD, ou=PKI, ou=DTRA Date: 2017.03.21 08:52:33 — 6a. DATE: Mar 21, 2017
7. PUBLIC AFFAIRS: KALOU — 7a. DATE: 3/24/17

8. TITLE: REVEAL-SCIPUFF Data Assimilation System Development and Demc — 9. CONTRACT NUMBER: HDTRA2-16-C-0001

10. COMPANY/GOVT LAB/ AUTHOR'S NAME: Aeris,LLC, Spectral, Sensor Solutions, & California State University-Chico

11. TYPE OF MATERIAL: ☐ PAPER ☒ PRESENTATION ☐ ABSTRACT ☐ OTHER

12. OVERALL CLASSIFICATION: ☐ CONTRACTOR RECOMMENDED CLASSIFICATION ☒ PROJECT OFFICER RECOMMENDED CLASSIFICATION Unclassified

A. Review authority for unclassified material is the responsibility of the PM. Your signature indicates the material has undergone technical and security review.

NEED TO USE CURRENT FORM

B. Warning Notices/Caveats: ☐ RD ☐ FRD ☐ CNWDI ☐ NATO RELEASABLE ☐ SUBJECT TO EXPORT CONTROL LAWS

C. Distribution Statement:

Unclassified/Distribution Statement A
J9/A&AS/Dan Dugan
March 21, 17

☒ A. Approved for public release; distribution is unlimited (unclassified papers only).

☐ B. Distribution authorized to U.S. Government agencies only; (check the following):

- ☐ Contractor Performance Evaluation
- ☐ Foreign Government Information
- ☐ Administrative or Operational Use
- ☐ Specific Authority
- ☐ Premature Dissemination
- ☐ Proprietary Information
- ☐ Test and Evaluation
- ☐ Software Documentation
- ☐ Critical Technology

DUGAN.DANIEL.L.1294115001 Digitally signed by DUGAN.DANIEL.L.1294115001 DN: c=US, o=U.S. Government, ou=DoD, ou=PKI, ou=CONTRACTOR, cn=DUGAN.DANIEL.L.1294115001 Date: 2017.03.21 08:48:03 -04'00'

☐ C. Distribution authorized to U.S. Government agencies and their contractors: (check the following):

- ☐ Critical Technology
- ☐ Specific Authority
- ☐ Administrative or Operational Use
- ☐ Software Documentation
- ☐ Foreign Government Information

☐ D. Distribution authorized to the Department of Defense and U.S. DoD Contractors only; (check the following):

- ☐ Foreign Government Information
- ☐ Critical Technology
- ☐ Administrative or Operational Use
- ☐ Software Documentation
- ☐ Foreign Government Information

☐ E. Distribution authorized to DoD Components only; (check the following):

- ☐ Administrative or Operational Use
- ☐ Premature Dissemination
- ☐ Critical Technology
- ☐ Foreign Government Information
- ☐ Direct Military Support
- ☐ Software Documentation
- ☐ Specific Authority
- ☐ Proprietary Information
- ☐ Test and Evaluation
- ☐ Contractor Performance Evaluation

☐ F. Further dissemination only as directed.

☐ X. Distribution authorized to U.S. Government agencies and private individuals or enterprises eligible to obtain export-controlled technical data in accordance with DoD Directive 5230.25 (unclassified papers only).

CLEARED MAR 24 2017 DTRA Public Affairs FOR PUBLIC RELEASE

JOXS REPRESENTATIVE OPSEC concurs w/ release Stampoulos 24 Mar 17

RECEIVED MAR 22 2017 BY: ...

13. MATERIAL TO BE: ☒ Presented ☐ Published Date Required: 03Nov2016

14. NAME OF CONFERENCE OR JOURNAL: 2016 CBW&CA Modeling symposium

15. REMARKS: Work performed and brief is funded under DTRA contract # HDTRA2-16-C-0001; 2016 CBW&CA Modeling symposium